

A review on Nanocomposites

Part 2: Machinability

Bao Le, first author

Mechanical and Construction Engineering Department
Northumbria University
Newcastle upon Tyne NE1 8ST, UK
bao.le@northumbria.ac.uk

Jibran Khaliq, second author

Mechanical and Construction Engineering Department
Northumbria University
Newcastle upon Tyne NE1 8ST, UK
jibran.khaliq@northumbria.ac.uk

Dehong Huo, third author

Mechanical Engineering, School of Engineering
Newcastle University
Newcastle upon Tyne NE1 7RU
dehong.huo@newcastle.ac.uk

Xiangyu Teng, fourth author

Mechanical Engineering, School of Engineering,
Newcastle University
Newcastle upon Tyne NE1 7RU
txy19910914@hotmail.com

Islam Shyha, fifth author¹

Mechanical and Construction Engineering Department
Northumbria University
Newcastle upon Tyne NE1 8ST, UK
islam.shyha@northumbria.ac.uk

¹ Corresponding author

ABSTRACT

Micromachining of nanocomposites is deemed to be a complicated process due to the anisotropic, heterogeneous structure and advanced mechanical properties of these materials associated with the size effects in micromachining. It leads to poorer machinability in terms of high cutting force, low surface quality and high rate of tool wear. The review on the mechanical properties of nanocomposites with the aim to investigate their effects on the nanocomposites micro-machinability has been addressed in part 1. In part 2 of this paper, the subsequent micro-machining processes are critically discussed based on relevant studies from both experimental and modelling approaches. The main findings and limitations of these micro-machining methods in processing nanocomposites have been highlighted together with future prospects.

Keywords: *nanocomposites; micromachining; manufacturing; materials; mechanical properties*

1. INTRODUCTION

Part 1 of this review paper has addressed relevant methods to fabricate nanocomposites. Some main mechanical properties such as tensile strength, Young's modulus, fracture strength and fracture toughness seemed to be improved due to the addition of nano-fillers. The efficiency of these reinforcements was seen to depend on the nature of fillers and matrixes, filler size, filler content and fabricating methods. The reinforcement of nanofillers was also analyzed based on some main approaches such as strengthening and toughening mechanisms. Some typical methods to fabricate nanocomposites have been also discussed. However, these micromachining techniques are seemed to be incapable of producing a final product with sufficient quality in terms of surface quality, dimensional accuracy). Therefore, mechanical micromachining techniques such as micro-drilling, micro-milling have been potentially considered as post-processing methods to meet these manufacturing requirements. Some applications that employing mechanical micromachining of nanocomposites

have been mentioned in part 1 and therefore, a comprehensive review on the machinability when micromachining of nanocomposites is required.

Mechanical micromachining exhibits high capabilities in terms of surface quality, dimension accuracy and wide range of materials. However, the addition of reinforcements leads to the complex structure of nanocomposites (multiple phases, homogeneity, anisotropy, etc.) and their advanced mechanical properties (high tensile properties, hardness, wear resistance, etc.) could reduce the machinability of these materials. Moreover, micromachining also complicates the material removal process since it contains some basic differences from conventional machining such as cutting edge radius, minimum-uncut chip thickness (MUCT), micro-structure that are generally called size effects. All of those factors make micromachining of nanocomposites difficult to accomplish. Additionally, there is a scarcity of data related to the micromachining of nanocomposites. That is the reason for only a few reports on micromachining of nanocomposites available in providing in-depth analyses on micromachining of nanocomposites.

2. MICROMACHINING OF NANOCOMPOSITES

2.1 Overview of micromachining

The motivation of product miniaturization with high precision is to make multifunctional products with lightweight, high mobility, less energy consumption and higher efficiency. Along with the discovery of advanced materials (i.e. superalloys, composites, ceramics, etc.) with outstanding ratios of strength to weight, the development of advanced machining techniques with ultra-high precision makes the miniaturization of components feasible.

Taniguchi [1] has modified machining advancement by the achievement of

machining accuracy from conventional machining (1 to 100 μm) to ultra-precision machining (1 nm) ([Figure 1](#)~~Figure 1~~). In other perspectives, micromachining has been defined by its product dimensions (at least two dimensions ranging from 1 to 500 μm) that are extremely small to be fabricated by conventional machining [2]. The difference between precision machining and micromachining is identified by their own objectives. While the precision machining highlights the machining accuracy with the ratio of size to tolerance higher than 10,000:1, the intent of micromachining is to make micro-parts that are typically in the range of 1 to 100 μm [3]. Micromachining is also defined by the uncut chip thickness measurement when it becomes smaller than the mean value of grain size [4] or in the range of 0.1 to 200 μm [5]. However, with the continuous development of machining, this border would be narrowed.

There are many micro-machining techniques with their own capabilities in terms of machining accuracy, part size, work-piece material and geometrical complexity. Classification in an attempt to identify the distinct principles between some basic micromachining process, generally based on whether micro-electromechanical systems (MEMS) or non-MEMS mechanism. MEMS are manufactured by micromachining processes which use lithography-based techniques to make the near net shape in semiconductors such as sensors, transducers, actuator, and other electrical devices on a silicon substrate. MEMS-based techniques are usually employed to fabricate the products in the sizes ranging from 1 to 100 μm . The remarkable advantages of these kinds of micro-manufacturing are high accuracy of machined products without burr formation on the machined edges, low cost and feasible mass-producing applications due to their short processing time. However, their applications are limited by work-piece material, mostly silicon, a small range of

metals and ceramics because of high requirements of materials for MEMs such as deposition ability in thin films, high definition and reproduction. In addition, the geometrical complexity of micro-components is also a considerable disadvantage of MEMs-based micromachining whilst they can only be effectively managed with 2D or 2.5D machined subjects. Micromechanical machining, on the other hand, is a miniaturized version of conventional machining that employs a geometrical micro cutting tool to remove material. Although MEMS can achieve smaller feature size, this adaption in micro-fabrication has high potential in terms of machining accuracy, surface quality, wide range of work-piece materials, and high complex geometry of products (3D). Moreover, the gap between macro and micro mechanical machining is also bridged while studying this approach [6, 7] by discussing size effect issues.

2.2 Size effect in micromachining

Although micromachining has the same principle with conventional machining in terms of material removal mechanism, there are, however, some critical differences due to size effects when adapting from macro to micro-scale machining. Size effects make the relationship between inputs (micromachining parameters) and outputs (surface quality, chip formation, cutting forces, tool wear) distinct to the conventional machining. Therefore, it could be seen that size effects are the key issues as well as the basis to explain the unusual aspects that micromachining processes have achieved [6, 8-12]. Size effects are the results of extrapolated-value aberration from macro to micromachining. These effects are expressed by the dramatic, nonlinear increase of specific energy when the uncut chip thickness decreases [13]. Experimental results to support this phenomenon have been achieved when metal and alloys were cut taking into consideration the ratio between MUCT to cutting edge radius [14-16]. The specific

cutting forces (k_c) in micro-milling are hyper-proportionally increased when micro-milling at a feed per tooth (f) value lower than tool edge radius (r_e) [15], especially when reaching grinding levels ($f/r_e=0.1$), the specific cutting force could achieve maximum value of 70 GPa ([Figure 2](#)).

In general, size effects in micromachining are related to different aspects that are usually neglected in conventional machining including:

- A dramatic non-linear increase of specific cutting force when the uncut chip thickness adapts the cutting edge radius
- A consideration of the microstructure effect on the machining process when cutting parameters (depth of cut, feed rate) adapt grain size or strengthening effects.
- A critical threshold so-called MUCT that sets the lowest limit for feasible cutting operation and decides the state of cutting mechanism (shearing, sliding or ploughing).
- A complex analysis of cutting force and surface roughness due to high spindle speeds, tool deflection/chatter and run-out [17].
- Different design of the microtool to ensure the rigidity and stable, high tool wear and tool failure possibility when miniatures tool parameters.
- Finally, the combination of those factors makes a comprehensive explanation for the differences in terms of surface generation between macro-machining and micromachining.

Based on that the above, those aspects will be expressed in more details in the following sections. However, the influences of size effects on micromachining have been still unobvious and need more experimental investigation to support [8]. The

most specific exhibition of size effect is the higher specific cutting energy in micromachining compared to macro-machining ([Figure 3](#)~~Figure-3~~).

2.2.1 Microstructure effect

In macro machining, when the material volume or the removal rate of the material for once route is relatively high, the material structure, in that case, is considered homogenous and isotropic. Although, it still has a certain tolerance in this assumption but could be acceptable due to the high ratio between tool edge radius and grain size. On the other hand, when micromachining using micro-tools, the tool edge radius approaches the grain size, homogenous and isotropic assumptions are no longer valid. Work-piece material structure is now considered as an assemblage of distinct grains with random distribution within the material system or anisotropic characteristic [9, 10, 18, 19]. Therefore, in this case, the cutting mechanism takes place by breaking each individual grain [9, 12, 16] that requires more specific cutting energies or forces and mean flow stress due to atom bonds ([Figure 4](#)~~Figure-4~~).

The effect of microstructure when micromachining has been clearly exhibited especially in the case of multi-phase material. Vogler et al. [20] have studied a mechanistic force modelling which using micro-structure mapping for the micro-end milling multi-phase ductile iron. It is observed that more than 35% cutting energy increase due to microstructural effects when micro-end-milling multiphase ductile iron and higher frequency of cutting forces in comparison with macro-machining. The cutting forces, as well as other cutting conditions, vary when the cutting tool moves along two adjacent grains that have different mechanical properties. A 'two-grain model' has been used to study the grain boundary influences on cutting forces [21] or surface generation [22]. In addition, elastic recover in micromachining is also an

important factor of microstructure effects [18]. Furukawa and Moronuki [23] gave some experimental results to support for the grain boundary effect on cutting force variation in single-phase and multiple-phase as well as in brittle and ductile materials (pure copper, aluminum alloy, PMMA, CaF₂, and germanium). Mian et al. [24] have conducted a comparative study when micro-milling single-phase material (AISI 1005 steel) and multi-phase material (AISI 1045 steel). They claimed that the surface quality after micro-milling AISI 1005 was better than AISI 1045 due to the minimization of the differential elastic recovery in single-phase material ([Figure 5](#)~~Figure 5~~). Micromachining of multi-phase materials also leads to the unbalance of plastic strain that contributes to low surface quality and high cutting force variation [25]. The burr formation at the grain boundary areas also leads to higher surface roughness when micromachining multi-phase material. This burr formation is due to chip formation interrupting when tool adapts the grain boundary [26]. Nevertheless, in general, the chip loads is recommended to be ten times higher than the grain size to obtain high surface quality [23].

Furthermore, it could be seen that a homogenous and isotropic material is considered the ideal condition for achieving high surface quality. This grain size effect has been indicated by Uhlmann et al. [27] when high machined surface, as well as hardness, could be positively affected by the high levels of material homogeneous property ([Figure 6](#)~~Figure 6~~). However, the surface roughness when micro-milling W/Cu 80/20 was still higher than W/Cu 75/25 that had a lower level of homogeneity. Popov et al. [28] have indicated that a remarkable improvement of surface quality can be feasible through the refinement of grain size to make higher homogeneity and isotropy and the grain size, in the case of micro-milling aluminum alloy, have a significant

influence on surface roughness. In details, with the decrease of the anisotropy and grain size of work-piece material from 100-200 μm into 0.6 μm , the surface roughness decreased more than three times compared to non-refinement material. They also suggested the optimal cutting condition with narrow grain distribution associated with certain cutting direction could achieve the highest quality of machined surface, but due to the limit of certain refinement process, this was still a target for further research. Lauro et al. [29] in the similar adaption, indicated that with the small grain size (39.9 μm), the variation of surface roughness will be reduced to 2% compared to larger grain size (51.1% when using grain size of 497 μm). Similar explanation about heterogeneous microstructure effect of multiphase material on surface roughness has been given by Weule et al. [18]. Therefore, it could be seen that reduce grain size tends to improve the machined surface quality and its role seems to be dominant in micromachining. Furthermore, the microstructure effect also exhibited by changing cutting directions and/or crystal orientation due to the anisotropic structure of materials when micromachining. Komanduri et al. [30] used a MD model to study cutting forces variation when specifically combining crystal orientation and cutting directions. To et al. [31] identified the higher surface quality can be achieved when micro-cutting single-crystal aluminum along (100) plane than (110) and (111) planes but Zhou and Ngoi [32] have claimed that the dominant factor was not cutting direction but the plastic behavior of single crystal. However, Moriwaki [19] neglected the effect of crystallographic orientation when micromachining polycrystalline copper. They claimed that surface quality degradation is caused by the formation of the amorphous damaged layer due to ploughing effect when the uncut chip thickness is at 0.1 μm . In general, the microstructure effects on the micro-machinability are indicated

by the inhomogeneity (grain size effect), anisotropic (different cutting directions) and structure (different phases) that lead to the variation of surface roughness, cutting forces and burr formations.

2.2.2 Minimum uncut chip thickness (MUCT) and cutting edge radius

The chip removal mechanism is among the principal differences between micro and conventional machining due to size effects. The contact between the cutting tool clearance face and work-piece surface is usually ignored and the tool edge is considered sharp in the case of macro-machining. It could be explained by the high ratio of the MUCT to cutting edge radius. When down-scaling into the micro-cutting mechanism, they become comparable to the tool edge radius and hence change the chip formation mechanism.

In micromachining, the MUCT could range from submicron to a few microns and the depth of cut and feed-rate varies from a few microns to maybe 100 μm , hence the cutting edge radius and the grain size become comparable [33]. In that case, tool edge radius becomes a dominant factor as well as feed-rate that affect the surface roughness. Moreover, the surface roughness tends to increase with the feed-rate decrease exceeds a lower minimum chip thickness [26]. (~~Figure 7~~Figure 7). That means MUCT has an inverse effect on surface roughness in case of micro-machining. A decrease of UCT into below the magnitude of edge radius (10-60 nm) leads to a significant increase of surface roughness for various levels of cutting speeds (10 and 150 m/min) [34]. In micromachining, shear stress increases around the cutting edge instead of along the shear plane [6, 9], and the work-piece is ploughed or elastically deformed rather than being sheared/cut [35, 36] when cutting depth and feed-rate below a threshold so-called 'minimum uncut chip thickness'. It was defined as a lower

limit of minimum under form chip thickness that can be feasible to be removed [37]

([Figure 8](#)~~Figure 8~~).

Another explanation for the negative effects of UCT on surface roughness is related to plastic deformation of materials during the machining process. It is observed that the surface quality is reduced when decreasing the ratio of UCT and edge radius is due to two reasons: first is the plastic accumulation of work-piece material on the tool surface [38] and the second reason is adhesive work-piece material on the machined surface [39] caused by material strengthening. Furthermore, the shear angle decreases along with the MUCT leading to deformation areas expanded and hence increasing the mean friction that negatively affects the surface quality.

Furthermore, elastic deformation of materials in micromachining is also negatively affected the surface quality. When the cutting depth adapts to the tool edge radius magnitude, the effective rake angle of micro-cutting tool transforms from positive to zero or even negative. This transformation makes the cutting more stable but also leads to some negative effects, such as more elastic deformation due to shear zone expanding, higher stress, strain, cutting forces, and energy consumption. It also leads to a high ratio of ploughing/shearing in the cutting mechanism, making the cutting mechanism becomes less efficient ([Figure 9](#)~~Figure 9~~). Therefore, the identification of MUCT in micromachining is significantly important to attain an optimal machining process. L'vov [40] considered the influence of MUCT as a function of the tool edge radius and recommended that the depth of cut should be above 29.3% of the tool edge radius to avoid ploughing and elastic deformation when micro-cutting SAE 1045 steel. Other researchers identified the minimum chip thickness by studying the cutting mechanism along with various feed rate levels in micro-milling 360 brass,

and the minimum chip thickness is approximately 30% of the tool edge radius [41]. Liu et al. [42] provided experimental results when identifying the ratios of chip thickness/tool edge radius λ_n (normalized minimum chip thickness) of 0.35-0.4 for micro-end-milling Al 6082-T6 and 0.2-0.3 for micro-end-milling AISI 1018 steel over a range of cutting velocity (84,000 to 150,000 rpm) and feed-rate (0.5 to 4 $\mu\text{m}/\text{flute}$).

In general, the size effects exhibited by the ratio of MUCT/cutting edge radius in the range of about 0.05 to 0.4 depending on materials and cutting parameters that have been supported by experimental, theoretical, and modelling results that were published in many studies when micromachining metals and alloys ([Table 1](#)~~Table 1~~).

2.3 Micro-milling of nanocomposites

Micromachining nanocomposites are significantly different from the process with metals, alloys. The low machinability due to their advanced mechanical properties and the extensive cutting conditions (extreme small MUCT and high cutting speed) are the main challenges when micromachining nanocomposites. In addition, the effects of heterogeneity, anisotropic of materials, volume fraction and distribution of nano-fillers make the cutting mechanism even more complicated. For example, Deng et al. [43] indicated that interface failure could contribute around 35% to cutting forces increase when micro-milling Al/45 vol.% SiC composites besides the shearing - ploughing factor. This part of the paper will be focused on the cutting mechanism when micromachining nanocomposites in terms of cutting forces, surface generation, chip morphology and tool wear. As mentioned, micromachining has been focused extensively on metals and their alloys while machining of nanocomposites, on the other hand, is still limited [44, 45]. The following sections will discuss in details the most common objectives of current researches related to micromachining of different

types of nanocomposites as well as their limitations.

2.3.1 Micro-milling of CNT-based nanocomposites

PMNCs are widely applied in micromachining due to their huge potential applications in industry. The mechanical, thermal and electrical properties of polymers are significantly improved when reinforcing with CNT that lead to the requirement of machinability investigation when micromachining these materials. In addition, the mechanical properties of CNT reinforced polymer nanocomposites (CNT/PMNCs) for instance: tensile strength, Young's modulus or hardness are considered feasible for mechanical micromachining applications hence make this study area more adaptable. Cutting force, surface roughness, chip formation, and tool wear are the most common objectives that take the effects of nanomaterial properties and cutting parameters into account.

Kumar et al. [46] have investigated the machinability when micro-milling PC/GNP/MWCNT nanocomposites in terms of cutting force, dimensional accuracy, chip morphology and surface roughness. Cutting forces were higher when micro-milling PC/GNP/MWCNT than plain PC (~ 22% at 4 μm /tooth feed rate) that suggesting the dominant of strengthening effects due to higher mechanical properties and the decrease of thermal softening effect due to the thermal conductivity improvement when reinforcing PC with MWCNT (and GNP).

The thermo-mechanical properties also lead to higher dimensional accuracy and surface quality (~197% at a feed rate of 3 μm /tooth) ([Figure 10](#)~~Figure 10~~) when micro-milling PC/GNP/MWCNT, especially at high feed rate where the effect of softening is minimized. These explanations were validated by the consideration of chip morphology with discontinuous forms when micro-milling PC/GNP/MWCNT that

reconfirmed the role of CNT in chip breakage. However, the effects of size effects, filler loading and cutting speed on the micro-machinability have not been addressed.

The chip formation due to the presence of CNT has also been investigated by Samuel et al. [45] with different forms and explanations. Instead of being broken, the chip formation tends to be continuous and curly when micro-milling PC/CNT nanocomposites for the entire range of feed rates. It is possibly due to the good rake face lubrication [47] that could attain from reducing the friction coefficient of CNT along the rake face in comparison with plain PC [48]. In addition, the presence of adiabatic shear bands on plain PC chip surfaces as well as their absence in case of PC/CNT indicated the effect of thermal conductivity of materials on chip morphology ([Figure 11](#)~~Figure 11~~).

Heat concentration at the cutting interface due to poor thermal properties also led to built-up-edge (BUE) formation on tool face, resulting in a poor surface finish in case of micro-milling plain PC as compared to PC/MWCNT nanocomposite ([Figure 12](#)~~Figure 12~~). In addition, the infestation of CNT and polymer smearing on the machined surface also contributed to its high surface quality. The cutting forces when micromachining PC/CNT nanocomposites were also lower in this case due to the reduction of shear strength for failure than plain PC or the low-quality bonding of PC-CNT [49], especially when high feed rates (shearing-dominated regime) were applied ([Figure 13](#)~~Figure 13~~). The lower friction coefficient of PC/CNT might also play a key role in cutting forces reduction [50] that has not been addressed by the authors. **Mahmoodi et al. [51]** also confirmed the important roles of thermal-mechanical properties and microstructure effects on cutting force variations. However, the experimental results showed higher cutting forces when micro-milling PC/MWCNT nanocomposite than

plain PC only when the feed rate ($2\ \mu\text{m}$) was lower than edge radius ($\sim 3\ \mu\text{m}$) as a result of ploughing dominance in cutting mechanism due to MUCT effects. Therefore, it could be seen that the strengthening effects seem to be dominant on cutting forces when size effects are taken into account. The effect of CNT orientation has been also investigated with the significant increase when micro-milling in the inflow direction as compared to the cross-flow direction ([Figure 14](#)~~Figure 14~~). It was explained based on strengthening-dominated effects due to higher thermos-mechanical properties of inflow nanocomposite. In addition, the surface quality of PC/MWCNT specimens after micro-milling seemed to be better than a plain PC. However, no experimental results or explanation related to surface roughness was given.

Stress concentration and crack formation ahead the tooltip due to CNT agglomeration were indicated the main reasons for cutting force reduction of cross-flow machining. The study has neglected the effects of filler content, cutting speed on the machinability when micromachining of nanocomposites as well as the investigation of chip formation that is necessary to support for the discussion. The influences of cutting speed on surface roughness when micromachining HDPE/MWCNT nanocomposites have been experimentally claimed less significant than feed rate [52] due to the obvious feed marks on the specimen surfaces but no detailed discussion was expressed. This has been reconfirmed by Zinati [and Razfar](#) [53] in an investigation on surface roughness with variations of cutting speed, feed rate and MWCNT content. The ANOVA analysis has also exhibited the least effect of filler loading on surface roughness generation. However, surface roughness variation, in this case, was only explained by tool-workpiece interaction when changing feed rates and cutting speeds without concerning about the thermo-mechanical properties of

PA6/MWCNT nanocomposites.

The effect of filler loading on the micro-machinability of polymer/CNT nanocomposites has been only investigated by Samuel et al. [44]. The study highlighted the basic role of CNT addition in different chip formations as well as a cutting mechanism when micro-milling PC/CNT nanocomposite and plain PC. Reinforcing CNT changed the stress-strain behavior of PC based materials, exhibiting by the reduction in strain-to-failure that indicated a ductile-to-brittle transition when the CNT loading reached to 5 wt.%. When micro-milling at low feed rates were applied, the chips were still continuously formed even in extremely low feed rate (0.3 $\mu\text{m}/\text{tooth}$) with high-content CNT nanocomposites (5 wt.%, 15 wt.%). The plain PC or PC/5 wt.% CNT, on the other hand, showed discontinuous chip formation. Therefore, it could be seen that the addition of CNT reduced the MUCTs of the PC/CNT nanocomposites that also indicated the size effects in micromachining. The improvement of machined surface quality associated with burr width reduction due to the addition of CNTs that leads to thermal conductivity improvement has been observed (especially at a high cutting speed of 130 m/min) with similar explanations as to their previous study [45] ([Figure 15](#)~~Figure 15~~).

However, CNT content did not show considerable influence on cutting force in this case. Its effect became less dominant with the increase of cutting speed that indicated high sensitivity of strain rate (cutting speed) regarding cutting force variation instead ([Figure 16](#)~~Figure 16~~). Cutting force exhibited significant reduction when increasing cutting speed regardless of the filler content, but the reasons for those changes were different between PC, PC/1.75% MWCNT and PC/5%MWCNT, PC/15%MWCNT.

While the advancement of cutting speed leads to the thermal softening-dominated regime of micromachining PC and the low-loading CNT, it is likely due to the interface failure or crack propagation from low interfacial bonding of CNT-PC when dealing with a higher content of CNT. The influence of heat transferring improvement due to the addition of CNT on cutting force when micromachining CNT reinforced polymer nanocomposites has been also investigated by Mahmoodi et al. [51]. Cutting force was considered as a function of cutting and edge coefficients in this case. The two main factors that were considered affecting these coefficients included: CNT content and CNT orientation. The radial and tangential have been considered as two components of cutting force ([Figure 17](#)~~Figure 17~~).

Optimization of instantaneous force method has been applied to identify the cutting force coefficient. Based on that, it could be seen that when micro-milling at feed rates below MUCT, cutting forces were much higher than that of higher feed rates due to the much higher values of ploughing coefficients than cutting coefficients. However, the experimental results from this study did not exhibit the same trend as expected with low cutting forces at a low feed rate (ploughing-dominated regime at feed rates below 2 μm). The influence of CNT orientation on cutting force has also been exhibited with slight reductions of cutting coefficients when changing from in-flow to cross-flow cutting that indicated lower values of cutting forces. However, there was also no experimental result to validate this propose. In general, the effect of CNT addition on micro-machinability in terms of improving thermo-mechanical properties of CNT based polymer nanocomposites has been seen as the most important factor. Associated with MUCT and microstructure effects, CNT addition influences the cutting mechanism and chip formation, hence affecting cutting force, surface roughness and

dimensional accuracy. However, recent studies have still exhibited different results (outputs) and the dominances of various input factors with distinct explanations ([Table 2](#)) that reconfirmed the high complexity when micromachining nanocomposites. In addition, most of those researches have been only focused on the effect of feed rate while the roles of CNT type, filler content, fiber orientation and a cutting tool were almost neglected. In terms of machinability, no study has addressed about tool wear that is a highly important criterion, especially in micromachining nanocomposites.

2.3.2 Micro-milling of graphene-based nanocomposites

Although graphene has high potential in terms of reinforcing various matrix materials such as polymers, metals or ceramics, it has been seen that few studies have investigated these graphene-based nanocomposites recently. One of the early studies about micro-machinability of graphene-based nanocomposite has employed graphene platelets (GPL) as the secondary filler [49]. The main objective of this study is to consider the differences in micromachining responses between two-phase composite (epoxy/GF) and three-phase composite (epoxy/GF/GPL). The addition of GPL has remarkably revealed a better micro-machinability of hierarchical composite in terms of lower cutting forces, surface roughness and tool wear than the baseline composite. It was explained by the improvement of thermal conductivity of epoxy when adding GPL and also the reduction of friction along with the tool-chip interface that reducing BUE of polymer and tool wear subsequently. This explanation is similar to that of the micromachining polymer/CNT nanocomposites that have been aforementioned. Moreover, the influences of GPL on reducing surface roughness have been also analyzed by considering the concept of effective fiber length ([Figure](#)

~~18Figure 18~~). It was explained by the enhancement of interfacial strength of GPL-epoxy, making a longer effective fiber length and subsequent shearing-dominated cutting regime. In the case of baseline composite (epoxy/glass), glass fiber tended to bend and extrude on chips and machined surfaces indicating the lower effective fiber length, subsequent bending-dominated regime. The effects cutting speed on machined surface roughness have also been concerned with preferable high cutting speed for both materials to attain low cutting forces and surface roughness but no explanation has been given. The effect of feed rate on the micro-machinability, however, has been not concerned (~~Figure 19Figure 19~~). The reduction of cutting force due to the effect of strain rate (cutting velocity) and MUCT because of GPL addition has been also investigated by Arora et al. [54] with similar discussion to the case of micro-milling PC/MWCNT [45]. The alternation of thermal softening and strain hardening due to ductile-to-brittle transition associating with minimum chip thickness effects have been applied to explain the cutting force variations when increasing cutting speed. However, a different trend in terms of cutting force variation could be seen between the two studies. From ~~Figure 20figure 20~~, it was observed that there were some fluctuations of cutting force when micro-milling epoxy and epoxy/GPL (0.1 wt.%) at low cutting speeds (7.5 – 17.5 mm/min) while they constantly decreased in case of PC/MWCNT. This difference comes from the different natures between epoxy (thermoset) and PC (thermoplastic) and the applied range of cutting speeds. In such low cutting speed, the thermal softening mechanism has not still taken effect on reducing cutting forces yet, especially with thermoset polymers (epoxy) that have higher heat resistance than thermoplastics (PC). Therefore, the ploughing cutting mechanism is now dominated at low feed rate (3 μm) instead that contributed to

cutting force increase. The lack of rising portion in case of epoxy/GPL (0.2 wt.%) might be due to the reduction of minimum chip thickness leading to the dominance of ploughing at lower cutting speeds (<7.5 mm/min). The highest cutting forces at 0.2 wt.% GPL were also due to the highest improvement in the mechanical properties of the nanocomposite. Tool wear has also been investigated in this study with the optimum when micro-milling at 0.2 wt.% of GPL due to the lubricant nature of GPL and its role in reducing the elastic recovery of the matrix phase. At higher loading of GPL, their agglomerations were considered to accelerate the tool wear [55].

However, the effect of graphene addition on dimensional accuracy when micromachining polymer-based nanocomposites have not been considered sufficiently. Among relevant studies, only Kumar et al. [46] discussed the improvement of dimensional accuracy when micro-milling PC/MWCNT in comparison with the plain matrix. The effect of thermo-mechanical properties is again the main reason for this phenomenon that leading to the strengthening-dominated mechanism when cutting CNT-based polymer nanocomposite instead of the thermal softening regime in that of its plain counterpart. In addition, an elevation of cutting force has been observed in this case that was different from the aforementioned studies. While adding graphene [49] or CNTs [45] have in polymer matrix have been indicated the main factor for cutting forces reduction due to two reasons: reduce friction coefficient in tool-chip interaction that lead to superior rake face lubrication and low interfacial failure strength between polymers and nano-fillers, this study, however, differently claimed a high specific surface area of GPL increasing tool-GPL interaction associated with its rough/wrinkled morphology enhancing mechanical interlock within PC matrix were two reasons that leading to cutting forces rise.

The strain-hardening-dominated effect when adding GPL into a polymer matrix that leads to high cutting force has also been confirmed by Arora et al. [54] at 0.2 wt.% GPL. Highest cutting forces confirm the most effective reinforcement of mechanical properties at a certain threshold of graphene content that if exceed this limit, the influence of filler agglomeration will accelerate crack propagation or reduce shear strength to failure of polymer-graphene bonding [56]. These different trends of cutting force variation in a consideration of graphene loading can be seen in [Figure 21](#)~~Figure 21~~. Similar to micromachining-polymer/CNT studies, the most common objectives of that in polymer/graphene are also about cutting force, surface roughness and chip formation.

On the other hand, tool wear has been received more attention in case of micromachining polymer/graphene nanocomposites [49, 54, 56] that indicated its importance as a machinability indicator. By discussing aforementioned studies, it could be seen that effects of graphene addition associated with cutting speed and feed rate have been considered changing the thermos-mechanical properties of the based polymer matrix, hence affecting the cutting mechanism, chip formation and subsequent cutting force, surface roughness and tool wear. However, the effect of material and geometry of micro-tool has not been investigated (

[Table 3](#)~~Table-3~~).

Other gaps related to micromachining of graphene-based nanocomposites proposing through the discussion of relevant studies are the lack of attention in micromachining metal matrix and ceramic matrix-based material. Only Gao and Jia [57] has proposed simulated results in terms of the standardized effects of various inputs (depth of cut, cutting speed, tool rake angle, edge radius, graphene content and

size) on cutting force only without sufficient explanations ([Figure 22](#)~~Figure 22~~).

2.3.3 Micromachining of nano-ceramic based nanocomposites

When polymer-based matrix nanocomposites have mostly been applied in micromachining that employing CNTs and graphene as nano-fillers, metallic materials, on the other hand, are the most common matrices that have received more attention in terms of their micro-machinability when reinforcing with nano-ceramic particles. It comes from the requirement to fabricate high-toughness, corrosion than their metallic counterparts. One of the early studies that have investigated the micro-machinability of metal/ceramic nanocomposites was published by [58] with the considerations of cutting force variations as a function of filler loading, feed rate and cutting speed while micro-milling Mg/SiC nanocomposites. Interestingly, the size effect has been applied to explain the non-linear correlation between specific cutting forces and feed rates with larger ploughing zone in case of micromachining Mg/SiC nanocomposite ([Figure 23](#)~~Figure 23~~). It is totally different from the case of micromachining polymer-based nanocomposites. The main reason is the predominance of thermal softening due to the reduction of thermal conductivity when micro-milling Mg/SiC at low feed rates. In addition, its high specific cutting energies in ploughing zone and high cutting forces also indicated the influences of strengthening and microstructure effects when micromachining inhomogeneous materials. Those influences also exhibited on the complex profiles of cutting force variations when micromachining Mg/SiC nanocomposite. The effect of filler content has been significantly affected cutting forces at 5-10 vol % of SiC due to its highest efficiency of reinforcement at this certain level [59] ([Figure 24](#)~~Figure 24~~) that was similar to some experimental results in case of micromachining of polymer/CNT [44] and polymer/GNP [54, 56]. The complex cutting

mechanisms in micro-range parameters due to other factors such as tool deflection or microstructure effect neglected the role of feed rate on surface roughness as well as leading unobvious correlations between filler content-cutting speed and surface roughness.

With micromachining of metal/ceramic nanocomposites, tool wear has been received more attention than that of CNT and graphene-based polymer nanocomposite. It is possibly due to the high improvement of corrosion resistance and mechanical properties of those nanocomposites due to the presence of nano-ceramic particles. Teng et al. [60], in a comparative study of micro-machinability between Mg/TiB₂ and Mg/Ti, have claimed the effect of nano-filler additions on tool wear as well as cutting force and surface quality. The roles of thermo-mechanical properties due to the presence of nano-fillers in micro-machinability of particle reinforced metal-based nanocomposites seem to be similar to polymer/CNT and polymer/graphene nanocomposites. It exhibited by the higher tool wear rate when micro-milling Mg/TiB₂ with tool coating peeling in comparison with that of Mg/Ti. Due to size effect, the associated effects of depth of cut (DoC) and feed rate on cutting force increase were only available in the shearing region. On the other hand, thermal softening-dominated effect when increasing cutting speed and DoC has been claimed the main reason for surface roughness variations. In addition, the high ductility of Mg/Ti led to more chip adherence on tool surface that increasing cutting forces and subsequent surface roughness. However, no explanation related to thermal softening or strain hardening effects was given as compared to [59] ([Figure 25](#)~~Figure-25~~). However, Xiong et al. [61] have claimed that feed rate had the most dominant effects on cutting force when micro-milling Al/TiB₂ instead of filler content or cutting speed due to their influences

on increasing shear angle and decreasing friction angle while Pramanik et al. [62] confirmed that the increase of material removal rate (MRR) at high feed rates contributed to cutting force escalation.

From the mentions of relevant studies above, it could be seen that the application of micromachining or the investigation of micro-machinability of nanocomposites mostly focused on three main materials: CNTs or graphene reinforced polymer matrix and nano-ceramic-particles reinforced MMNCs. While micromachining the first two materials have similar features due to the similarities between CNTs and graphene properties, the last one exhibited different trends of micro-machinability, especially chip formation and cutting force. A summary of relevant studies of micromachining of nano- ceramic-particles MMNCs is given in [Table 4](#)~~table 4~~. In addition, while chip formation has been extensively concerned in case of micromachining polymer-based nanocomposites, cutting force variation, on the other hand, was the main objective of micromachining metal matrix based nanocomposites. Those aforementioned differences are possibly due to the different natures between polymer and metal matrices as well as the distinct reinforcement nature of nano-ceramic particles as compared to CNTs or graphene (geometry, thermos-mechanical properties). For instance, it made the role of thermal conductivity in case of micromachining metal matrix less dominant than polymer matrix while the role of strengthening mechanism become more significant. It is also necessary to be mentioned that mechanical micromachining on ceramic-based nanocomposites have not been applied recently although there was one study has mentioned about micromachining SiO₂/GNPs nanocomposite using EDM [63]. It possibly due to advanced mechanical properties of ceramic-based nanocomposites that lead to

extreme low micro-machinability (high tool wear, cutting force or low surface quality) or severity cutting operations.

Based on the discussion of relevant studies, it could be seen that micromachining of nanocomposites is a complicated process with the associations of many factors such as microstructure effects, MUCT, cutting edge radius or the thermo-mechanical properties of nanocomposites ([Figure 26](#)~~Figure-26~~).

In general, the influences of nano-fillers on micro-machinability of nanocomposites have been confirmed while feed rate, cutting speed, depth of cut have exhibited some different effects on machinability of nanocomposites from conventional machining in some specific cases due to size effect. However, the number of studies in terms of micromachining nanocomposites have been limited, mostly focus on CNTs or graphene reinforced polymer matrix or nano-ceramic particles reinforced MMNCs. It leads to a lack of sufficient information to analyze the micro-machinability variations of these materials.

2.4 Other processes for micromachining nanocomposites

Unlike micro-milling, the investigations of micro-manufacturing of nanocomposites using other techniques have been less extensive. There were few studies discussed micromachining of nanocomposites that employing micro-drilling, micro-EDM and laser micromachining. The exiting literature provided insufficient details to have a comprehensive evaluation of these techniques when machining of nanocomposites. For example, micro-drilling of composites has only concerned about drilling delamination and thermal damage in polymer nanocomposites. Li et al. [64] claimed that the inter-laminar fracture toughness of microwave cured MWCNT/CF/Epoxy was higher than that of the tradition cured CF/Epoxy composites. It

also led to a reduction of delamination factor (16%). Regarding the thermal damage during the micro-drilling process, the experimental results showed a maximum temperature of 23°C which was lower than that of the traditional composites and below the glass transition temperature of the epoxy matrix. It led to the minimization of thermal damage during machining process due to the addition of MWCNT. A similar improvement of laminar stiffness and reduction of delamination factor could be found in [65] when micro-drilling carbon nano-fiber reinforced with CFRP nanocomposites compared to its conventional composites (without CNF). In addition, Bello et al. [66] also investigated the exposures of nano-fibers during micro-drilling CNT-hybrid nanocomposites using multiple real-time instruments to characterize. In general, most of the aforementioned relevant studies only engaged in micro-drilling of hybrid nanocomposites in which the additional of nano-fillers were considered as hierarchical reinforcement to support for the reduction of delamination of conventional CFRPs.

For laser micromachining, the most common objective was material ablation as a function of laser fluency. Lu et al. [67] conducted some experiments using laser micromachining to fabricate micro-holes (diameter of 40 μm) from HPDE/CNF nanocomposite. They claimed that the addition of CNFs significantly enhanced the polymer decomposition, hence improving the ablation process. The additional of CNT also led to grain size refinement, thermal conductivity enhancement and reduction of light transmittance of ceramic-based nanocomposites. Therefore, the ablation depth and machined surface integrity were significantly improved. Das et al. [68] also showed that laser micromachining of epoxy/BaTiO₃ nanocomposites could generate suitable surfaces from multifunctional capacitor applications when a frequency-tripled Nd: Y AG laser operating at 355 nm wavelength. The available literature on relevant studies

of micromachining of nanocomposites using micro-drilling, laser micromachining and micro-EDM are given in [Table 5](#)~~table-5~~.

3. MODELLING OF MICROMACHINING OF NANOCOMPOSITES

There are various models available to analyze the machinability of nanocomposites using micromachining. Those models include analytical [69, 70], mechanistic models [20], finite element models [71] and MD models [72, 73]. The analytical models simulate the machining responses based on analytical solutions of mathematical modelling [70, 74] however their results are not really accurate. The mechanistic models provide the machine responses by investigated material [75, 76], however, require validations from experiments that more complex with various content of nano-fillers. MD simulations are applied in micromachining [77, 78] however due to limitations of time/length-scale, computational effort, and complex formulas, they seem to be unsuitable for a high number of atom models [79]. On the other hand, finite element (FE) is one of the most common methods that has been applied in micromachining [80, 81]. The different materials of both tool and work-piece are capable to be assigned. Furthermore, this method is also suitable for multi-phase material (e.g. nanocomposites) in predicting cutting forces, stress, strain, temperature distribution, chip formation and tool wear.

A microstructure-level model to simulate the micromachining process of polycarbonate reinforced with CNT has been applied by DeVor and Kapoor [82] appeared to accurately predict cutting forces (error 8%), thrust force (error 13.4%) and chip thickness (error 10%). In general, the material structure was separated into main phases: matrix (PC) and reinforcing (CNT) phase. Based on the TEM images of the

nanocomposites, the CNT distribution within the matrix would be characterized for length, curvature, slope, and orientation [83]. Similarly, the failure modes were also separately identified for two phases. Plastic stretch was applied as the ductile failure and hydrostatic tension was employed for brittle failure [84-87] in the matrix phase while a simple strain-to-fracture was used for CNT failure.

The results of chip formations, subsurface damage of the simulation can be seen in [Figure 27](#)~~figure-27~~. Based on that, Jiang *et al.* [88] have developed a new microstructure-level model in micromachining polymer reinforced CNT nanocomposite. The principal difference was that they indicated the failure mechanism of the micromachining process was primarily affected by the CNT- polymer interface. This idea was supported by subsequent numerical and experimental results from [89, 90]. Therefore, this polymer-CNT interface should be modelled as a third phase in nanocomposite structure related to the load transfer from matrix to reinforcing phase [83, 91]. They also showed that the characterization of the interface properties was based on two main parameters: strength and fracture energy. Some nano-indentation tests have been conducted to identify these values. [Figure 28](#)~~Figure 28~~ shows the simulation results of this model. Other similar adaption in terms of simulation of micromachining polymer reinforced CNT has been conducted by Kumar *et al.* [46] in an attempt to investigate the heterogeneity of polymer-based nanocomposite with the addition of graphene. The PC matrix properties were characterized by Johnson-Cook (JC) constitutive material model [92] with the consideration of flow stress at high temperature and high strain rates.

The value of JC coefficients was provided by Dwivedi *et al.* [93]. The failure mode of the PC matrix was ductile damage for material separation and chip formation.

The filler (GNP) was considered isotropic [94]. The mechanical characterization was identified from the experimental validation of Tiejun *et al.* [95]. From the simulation, the chip formation and cutting forces seemed to be similar to the experimental results. Discontinuous chip due to the presence of GNP seemed to appear in the PC-GNP interface that was supposed to be the weakest location. In addition, the strengthening effect due to the addition of GNP led to higher cutting force when micro-milling PC/GNP nanocomposites. Although there were some differences between simulated and experimental results due to various filler distributions, the model was indicated to be able to simulate the chip morphology and the trend of cutting forces accurately ([Figure 29](#)~~Figure-29~~). Teng *et al.* [71] have developed other FE model that employed the same filler (nano Sic particles) of 1.5 vol% when considering the effect of uncut chip thickness and cutting edge radius on cutting force and chip morphology. It was concluded that the cutting forces in simulation increased along with the uncut chip thickness. However, the percentage error seemed to be higher at low uncut chip thickness and only improved when its value exceeded 0.1 μm . The lower values of simulated results in terms of cutting force were due to the assumptions such as sharp cutting edge, rigid cutting tool and without tool wear consideration. Similarly, the chip formation was also different while changing the uncut chip thickness. When the uncut chip thickness was from 0.1 to 0.2 μm , the chip formation could not take place due to ploughing with elastic deformation. Exceed that limit, the chip was formed irregularly that could be seen as the minimum chip thickness at about 0.5 μm (0.5R) ([Figure 30](#)~~Figure-30~~). In their later work [96], two FE models were established to comparing the machinability between micro-particles and nano-particles reinforced MMCs in terms of stress/strain distribution within work-piece, chip formation, surface

generation and tool wear. It was found that the particles reinforced within matrix act as a barrier restricting the stress propagation during the machining process ([Figure 31](#)~~Figure 31~~). The nano-particles were found to be intact during the machining process which is different from the micro-sized reinforced counterpart. It was explained by the better mobility of nano-particles caused by the significantly reduced particle size which bear evenly distributed stress and less kinetic energy.

4. CONCLUSIONS

Based on the relevant studies that have been aforementioned, it has been observed that although most nanocomposites fabrication and characterization have been conducted and discussed [in part 1](#), their applications and machinability investigations in micromachining have still been limited, predominantly to the polymer matrix and metal matrix and nanocomposites reinforced by CNTs, graphene or ceramic nano-particle reinforced. It is possibly due to some main reasons including their micromachining applications, material integrity/defect, micromachining feasibility (tool wear, vibration, etc.) and most importantly, the high complexity of micromachining nanocomposites.

Micromachining nanocomposite materials are more challenging compared to conventional machining process and bulk materials (e.g. metals, alloys and composites). The associations of many factors prominently effect of microstructure (homogeneity, anisotropic, grain size), improvements of thermo-mechanical properties (filler distribution, loading) of nanocomposites and size effects of micromachining complicate the manufacturing process as well as significantly decrease the machinability of these materials. In the case of fiber reinforcement, the

distribution of nano-fiber (e.g. CNT) and fiber/cutting orientation were also important factors in micromachining. Subsequently, the intricate micromachining process leads to unobvious relations between variable inputs such as feed rate, cutting speed and corresponding outputs (e.g. cutting force, surface roughness, chip formation) with different explanations. In some cases, the cutting parameters showed the inverse influences on the machinability compared to other conventional machining processes. Most studies have been concerned about the effects of filler content, feed rate and cutting speed on chip formation, cutting force and surface roughness. However, the effects of micro-cutting tool (material, geometry) and tool wear on micro-machinability of nanocomposites have been less investigated. In addition, the analysis of size effect when micromachining nanocomposites have been still under-researched although it has been addressed extensively when micromachining metals and alloys.

Nevertheless, through the discussion of both mechanical properties and mechanical micromachining of nanocomposites, a general view about their micro-machinability has been given. It would be the basic knowledge for further studies in this area in future. However, the gap of knowledge has also led to the requirement for more efforts for collecting quantitative data and sufficient information on this area.

The future research trends may suggest that micromachining of ceramic matrix nanocomposites should be addressed. Moreover, despite micromachining of nanocomposites has huge potentials to apply in industry, the state of the art in this field has shown very limited applications and most of them were in the prototyping stage. Therefore, the future researches could also focus on commercial applications of micromachining of nanocomposites.

REFERENCES

- [1] N. Taniguchi, "Current status in, and future trends of, ultraprecision machining and ultrafine materials processing," *CIRP Annals-Manufacturing Technology*, vol. 32, pp. 573-582, 1983.
- [2] G. Byrne, D. Dornfeld, and B. Denkena, "Advancing cutting technology," *CIRP Annals-Manufacturing Technology*, vol. 52, pp. 483-507, 2003.
- [3] M. P. Groover, D. Belson, A. Kusiak, J. M. Sánchez, J. W. Priest, L. J. Burnell, *et al.*, "Handbook of design, manufacturing and automation," 1994.
- [4] A. Simoneau, E. Ng, and M. Elbestawi, "Chip formation during microscale cutting of a medium carbon steel," *International Journal of Machine Tools and Manufacture*, vol. 46, pp. 467-481, 2006.
- [5] T. Masuzawa and H. Tönshoff, "Three-dimensional micromachining by machine tools," *CIRP Annals-Manufacturing Technology*, vol. 46, pp. 621-628, 1997.
- [6] J. Chae, S. Park, and T. Freiheit, "Investigation of micro-cutting operations," *International Journal of Machine Tools and Manufacture*, vol. 46, pp. 313-332, 2006.
- [7] D. Huo, *Micro-cutting: fundamentals and applications*: John Wiley & Sons, 2013.
- [8] A. Mian, N. Driver, and P. Mativenga, "Identification of factors that dominate size effect in micro-machining," *International Journal of Machine Tools and Manufacture*, vol. 51, pp. 383-394, 2011.
- [9] X. Sun and K. Cheng, "Micro-/Nano-Machining through Mechanical Cutting," *Micromanufacturing Engineering and Technology*, pp. 24-38, 2010.
- [10] D. Dornfeld, S. Min, and Y. Takeuchi, "Recent advances in mechanical micromachining," *CIRP Annals-Manufacturing Technology*, vol. 55, pp. 745-768, 2006.
- [11] M. C. Shaw, "The size effect in metal cutting," *Sadhana*, vol. 28, pp. 875-896, 2003.
- [12] M. Câmara, J. C. Rubio, A. Abrão, and J. Davim, "State of the art on micromilling of materials, a review," *Journal of Materials Science & Technology*, vol. 28, pp. 673-685, 2012.
- [13] F. Vollertsen, "Categories of size effects," *Production Engineering*, vol. 2, p. 377, 2008.
- [14] I. Kang, J. Kim, and Y. Seo, "Investigation of cutting force behaviour considering the effect of cutting edge radius in the micro-scale milling of AISI 1045 steel," *Proceedings of the Institution of Mechanical Engineers, Part B: Journal of Engineering Manufacture*, vol. 225, pp. 163-171, 2011.
- [15] F. B. de Oliveira, A. R. Rodrigues, R. T. Coelho, and A. F. de Souza, "Size effect and minimum chip thickness in micromilling," *International Journal of Machine Tools and Manufacture*, vol. 89, pp. 39-54, 2015.
- [16] A. Aramcharoen and P. Mativenga, "Size effect and tool geometry in micromilling of tool steel," *Precision Engineering*, vol. 33, pp. 402-407, 2009.
- [17] X. Lu, Z. Jia, S. Liu, K. Yang, Y. Feng, and S. Y. Liang, "Chatter Stability of Micro-Milling by Considering the Centrifugal Force and Gyroscopic Effect of the Spindle," *Journal of Manufacturing Science and Engineering*, vol. 141, 2019.
- [18] H. Weule, V. Hüntrup, and H. Tritschler, "Micro-cutting of steel to meet new requirements in miniaturization," *CIRP Annals-Manufacturing Technology*, vol. 50, pp. 61-64, 2001.
- [19] T. Moriwaki, "Machinability of copper in ultra-precision micro diamond cutting," *CIRP Annals-Manufacturing Technology*, vol. 38, pp. 115-118, 1989.
- [20] M. P. Vogler, R. E. DeVor, and S. G. Kapoor, "Microstructure-level force prediction model for micro-milling of multi-phase materials," *Journal of Manufacturing Science and Engineering*, vol. 125, pp. 202-209, 2003.
- [21] S. Venkatachalam, O. Fergani, X. Li, J. G. Yang, K.-N. Chiang, and S. Y. Liang, "Microstructure effects on cutting forces and flow stress in ultra-precision machining of polycrystalline brittle materials," *Journal of Manufacturing Science and Engineering*, vol. 137, p. 021020, 2015.
- [22] S. Shimada, N. Ikawa, H. Tanaka, and J. Uchikoshi, "Structure of micromachined surface simulated by molecular dynamics analysis," *CIRP Annals-Manufacturing Technology*, vol. 43,

- pp. 51-54, 1994.
- [23] Y. Furukawa and N. Moronuki, "Effect of material properties on ultra precise cutting processes," *CIRP Annals-Manufacturing Technology*, vol. 37, pp. 113-116, 1988.
- [24] A. J. Mian, N. Driver, and P. T. Mativenga, "A comparative study of material phase effects on micro-machinability of multiphase materials," *The International Journal of Advanced Manufacturing Technology*, vol. 50, pp. 163-174, 2010.
- [25] A. Simoneau, E. Ng, and M. Elbestawi, "Surface defects during microcutting," *International Journal of Machine Tools and Manufacture*, vol. 46, pp. 1378-1387, 2006.
- [26] M. P. Vogler, R. E. DeVor, and S. G. Kapoor, "On the modeling and analysis of machining performance in micro-endmilling, part I: surface generation," *J. Manuf. Sci. Eng.*, vol. 126, pp. 685-694, 2004.
- [27] E. Uhlmann, S. Piltz, and K. Schauer, "Micro milling of sintered tungsten-copper composite materials," *Journal of Materials Processing Technology*, vol. 167, pp. 402-407, 2005.
- [28] K. B. Popov, S. S. Dimov, D. T. Pham, R. Minev, A. Rosochowski, and L. Olejnik, "Micromilling: material microstructure effects," *Proceedings of the Institution of Mechanical Engineers, Part B: Journal of Engineering Manufacture*, vol. 220, pp. 1807-1813, 2006.
- [29] C. H. Lauro, S. L. M. Ribeiro Filho, A. L. Christoforo, and L. C. Brandão, "Influence of the austenite grain size variation on the surface finishing in the micromilling process of the hardened AISI H13steel," *Matéria (Rio de Janeiro)*, vol. 19, pp. 235-246, 2014.
- [30] R. Komanduri, N. Chandrasekaran, and L. Raff, "MD Simulation of nanometric cutting of single crystal aluminum-effect of crystal orientation and direction of cutting," *Wear*, vol. 242, pp. 60-88, 2000.
- [31] S. To, W. Lee, and C. Chan, "Ultraprecision diamond turning of aluminium single crystals," *Journal of materials processing technology*, vol. 63, pp. 157-162, 1997.
- [32] M. Zhou and B. Ngoi, "Effect of tool and workpiece anisotropy on microcutting processes," *Proceedings of the Institution of Mechanical Engineers, Part B: Journal of Engineering Manufacture*, vol. 215, pp. 13-19, 2001.
- [33] X. Liu, R. E. DeVor, S. Kapoor, and K. Ehmann, "The mechanics of machining at the microscale: assessment of the current state of the science," *Journal of manufacturing science and engineering*, vol. 126, pp. 666-678, 2004.
- [34] C. K. Ng, S. N. Melkote, M. Rahman, and A. S. Kumar, "Experimental study of micro-and nano-scale cutting of aluminum 7075-T6," *International Journal of Machine Tools and Manufacture*, vol. 46, pp. 929-936, 2006.
- [35] F. Ducobu, E. Rivière-Lorphèvre, and E. Filippi, "Chip formation in Micro-cutting," *J Mech Eng Autom*, vol. 3, pp. 441-448, 2013.
- [36] K. Woon and M. Rahman, "Extrusion-like chip formation mechanism and its role in suppressing void nucleation," *CIRP Annals-Manufacturing Technology*, vol. 59, pp. 129-132, 2010.
- [37] N. Ikawa, S. Shimada, and H. Tanaka, "Minimum thickness of cut in micromachining," *Nanotechnology*, vol. 3, p. 6, 1992.
- [38] K. Liu and S. N. Melkote, "Finite element analysis of the influence of tool edge radius on size effect in orthogonal micro-cutting process," *International Journal of Mechanical Sciences*, vol. 49, pp. 650-660, 2007.
- [39] G. Bissacco, H. N. Hansen, and L. De Chiffre, "Size effects on surface generation in micro milling of hardened tool steel," *CIRP Annals-Manufacturing Technology*, vol. 55, pp. 593-596, 2006.
- [40] N. L'vov, "Determining the minimum possible chip thickness," *Machines & Tooling*, vol. 4, p. 45, 1969.
- [41] C.-J. Kim, J. R. Mayor, and J. Ni, "A static model of chip formation in microscale milling," *Transactions of the ASME-B-Journal of Manufacturing Science and Engineering*, vol. 126, pp. 710-718, 2004.
- [42] X. Liu, R. DeVor, and S. Kapoor, "An analytical model for the prediction of minimum chip thickness in micromachining," *Journal of manufacturing science and engineering*, vol. 128, pp. 474-481, 2006.
- [43] B. Deng, L. Zhou, F. Peng, R. Yan, M. Yang, and M. Liu, "Analytical model of cutting force in micromilling of particle-reinforced metal matrix composites considering interface failure," *Journal of Manufacturing Science and Engineering*, vol. 140, 2018.
- [44] J. Samuel, A. Dikshit, R. E. DeVor, S. G. Kapoor, and K. J. Hsia, "Effect of carbon nanotube (CNT) loading on the thermomechanical properties and the machinability of CNT-reinforced polymer

- composites," *Journal of Manufacturing Science and Engineering*, vol. 131, p. 031008, 2009.
- [45] J. Samuel, R. E. DeVor, S. G. Kapoor, and K. J. Hsia, "Experimental investigation of the machinability of polycarbonate reinforced with multiwalled carbon nanotubes," *Journal of Manufacturing Science and Engineering*, vol. 128, pp. 465-473, 2006.
- [46] M. N. Kumar, M. Mahmoodi, M. TabkhPaz, S. Park, and X. Jin, "Characterization and micro end milling of graphene nano platelet and carbon nanotube filled nanocomposites," *Journal of Materials Processing Technology*, vol. 249, pp. 96-107, 2017.
- [47] J. Horne, "A new model for initial chip curl in continuous cutting," *International Journal of Mechanical Sciences*, vol. 20, pp. 739-745, 1978.
- [48] K. Enomoto, T. Yasuhara, S. Kitakata, H. Murakami, and N. Ohtake, "Frictional Properties of Carbon Nanofiber Reinforced Polymer Matrix Composites," *New Diamond and Frontier Carbon Technology*, vol. 14, pp. 11-20, 2004.
- [49] B. Chu, J. Samuel, and N. Koratkar, "Micromilling responses of hierarchical graphene composites," *Journal of Manufacturing Science and Engineering*, vol. 137, p. 011002, 2015.
- [50] H. Gopalakrishna, J. S. Rao, S. N. Kumar, V. V. Shetty, and K. Rai, "Effect of Friction on the Cutting Forces in High Speed Orthogonal Turning of Al 6061-T6."
- [51] M. Mahmoodi, M. Mostofa, M. Jun, and S. S. Park, "Characterization and micromilling of flow induced aligned carbon nanotube nanocomposites," *Journal of Micro and Nano-Manufacturing*, vol. 1, 2013.
- [52] Y. Gong, Y.-J. Baik, C. P. Li, C. Byon, J. M. Park, and T. J. Ko, "Experimental and modeling investigation on machined surfaces of HDPE-MWCNT polymer nanocomposite," *The International Journal of Advanced Manufacturing Technology*, vol. 88, pp. 879-885, 2017.
- [53] R. F. Zinati and M. Razfar, "Experimental and modeling investigation of surface roughness in end-milling of polyamide 6/multi-walled carbon nano-tube composite," *The International Journal of Advanced Manufacturing Technology*, vol. 75, pp. 979-989, 2014.
- [54] I. Arora, J. Samuel, and N. Koratkar, "Experimental investigation of the machinability of epoxy reinforced with graphene platelets," *Journal of Manufacturing Science and Engineering*, vol. 135, p. 041007, 2013.
- [55] A. Marcon, S. Melkote, K. Kalaitzidou, and D. DeBra, "An experimental evaluation of graphite nanoplatelet based lubricant in micro-milling," *CIRP annals*, vol. 59, pp. 141-144, 2010.
- [56] I. Shyha, G. Y. Fu, D. H. Huo, B. Le, F. Inam, M. S. Saharudin, *et al.*, "Micro-Machining of Nano-Polymer Composites Reinforced with Graphene and Nano-Clay Fillers," in *Key Engineering Materials*, 2018, pp. 197-205.
- [57] C. Gao and J. Jia, "Factor analysis of key parameters on cutting force in micromachining of graphene-reinforced magnesium matrix nanocomposites based on FE simulation," *The International Journal of Advanced Manufacturing Technology*, vol. 92, pp. 3123-3136, 2017.
- [58] J. Liu, J. Li, Y. Ji, and C. Xu, "Investigation on the effect of SiC nanoparticles on cutting forces for micro-milling magnesium matrix composites," in *ASME 2011 International Manufacturing Science and Engineering Conference*, 2011, pp. 525-536.
- [59] J. Li, J. Liu, and C. Xu, "Machinability study of SiC nano-particles reinforced magnesium nanocomposites during micro-milling processes," in *ASME 2010 International Manufacturing Science and Engineering Conference*, 2010, pp. 391-398.
- [60] X. Teng, D. Huo, E. Wong, G. Meenashisundaram, and M. Gupta, "Micro-machinability of nanoparticle-reinforced Mg-based MMCs: an experimental investigation," *The International Journal of Advanced Manufacturing Technology*, vol. 87, pp. 2165-2178, 2016.
- [61] Y. Xiong, W. Wang, R. Jiang, and K. Lin, "A study on cutting force of machining in situ TiB₂ particle-reinforced 7050Al alloy matrix composites," *Metals*, vol. 7, p. 197, 2017.
- [62] A. Pramanik, A. Basak, Y. Dong, S. Shankar, and G. Littlefair, "Milling of nanoparticles reinforced Al-based metal matrix composites," *Journal of Composites Science*, vol. 2, p. 13, 2018.
- [63] F. Zeller, C. Müller, P. Miranzo, and M. Belmonte, "Exceptional micromachining performance of silicon carbide ceramics by adding graphene nanoplatelets," *Journal of the European Ceramic Society*, vol. 37, pp. 3813-3821, 2017.
- [64] N. Li, Y. Li, J. Zhou, Y. He, and X. Hao, "Drilling delamination and thermal damage of carbon nanotube/carbon fiber reinforced epoxy composites processed by microwave curing," *International Journal of Machine Tools and Manufacture*, vol. 97, pp. 11-17, 2015.
- [65] I. P. T. Rajakumar, P. Hariharan, and I. Srikanth, "A study on monitoring the drilling of polymeric nanocomposite laminates using acoustic emission," *Journal of Composite Materials*, vol. 47,

- pp. 1773-1784, 2013.
- [66] D. Bello, B. L. Wardle, J. Zhang, N. Yamamoto, C. Santeufemio, M. Hallock, *et al.*, "Characterization of exposures to nanoscale particles and fibers during solid core drilling of hybrid carbon nanotube advanced composites," *International journal of occupational and environmental health*, vol. 16, pp. 434-450, 2010.
- [67] Y. Lu, D. Shao, and S. Chen, *Nanoparticle-enhanced laser micromachining of polymeric nanocomposites*: Society of Manufacturing Engineers, 2000.
- [68] R. N. Das, F. D. Egitto, J. M. Lauffer, and V. R. Markovich, "Laser micromachining of nanocomposite-based flexible embedded capacitors," in *2007 Proceedings 57th Electronic Components and Technology Conference*, 2007, pp. 435-441.
- [69] E. Lee and B. Shaffer, *The theory of plasticity applied to a problem of machining*: Division of Applied Mathematics, Brown, 1949.
- [70] M. E. Merchant, "Mechanics of the metal cutting process. I. Orthogonal cutting and a type 2 chip," *Journal of applied physics*, vol. 16, pp. 267-275, 1945.
- [71] X. Teng, D. Huo, W. Chen, E. Wong, L. Zheng, and I. Shyha, "Finite element modelling on cutting mechanism of nano Mg/SiC metal matrix composites considering cutting edge radius," *Journal of Manufacturing Processes*, vol. 32, pp. 116-126, 2018.
- [72] Z. Huang, Z. Guo, X. Chen, T. Yue, S. To, and W. Lee, "Molecular dynamics simulation for ultrafine machining," *Materials and Manufacturing Processes*, vol. 21, pp. 393-397, 2006.
- [73] R. Komanduri, M. Lee, and L. Raff, "The significance of normal rake in oblique machining," *International Journal of Machine Tools and Manufacture*, vol. 44, pp. 1115-1124, 2004.
- [74] M. Field and M. E. Merchant, "Mechanics of formation of the discontinuous chip in metal cutting," *Trans. ASME*, vol. 71, p. 421, 1949.
- [75] H.-J. Fu, R. DeVor, and S. Kapoor, "A mechanistic model for the prediction of the force system in face milling operations," *Journal of engineering for industry*, vol. 106, pp. 81-88, 1984.
- [76] R. DeVor and W. Kline, "A mechanistic model for the force system in end milling with application to machining airframe structures," in *Manufacturing Engineering Transactions and North American Manufacturing Research Conference, 8 th*, 1980, pp. 297-303.
- [77] K. Maekawa and A. Itoh, "Friction and tool wear in nano-scale machining—a molecular dynamics approach," *Wear*, vol. 188, pp. 115-122, 1995.
- [78] Z.-C. Lin and J.-C. Huang, "A nano-orthogonal cutting model based on a modified molecular dynamics technique," *Nanotechnology*, vol. 15, p. 510, 2004.
- [79] M. M. Shokrieh and R. Rafiee, "On the tensile behavior of an embedded carbon nanotube in polymer matrix with non-bonded interphase region," *Composite Structures*, vol. 92, pp. 647-652, 2010.
- [80] S. Park, S. G. Kapoor, and R. E. DeVor, "Microstructure-level model for the prediction of tool failure in WC-Co cutting tool materials," *Journal of manufacturing science and engineering*, vol. 128, pp. 739-748, 2006.
- [81] L. Chuzhoy, R. DeVor, S. Kapoor, and D. Bammann, "Microstructure-level modeling of ductile iron machining," *Journal of manufacturing science and engineering*, vol. 124, pp. 162-169, 2002.
- [82] R. DeVor and S. Kapoor, "Microstructure-Level Machining Simulation of Carbon Nanotube Reinforced Polymer Composites—Part I: Model Development and Validation," *Urbana*, vol. 51, p. 61801, 2008.
- [83] A. Dikshit, "A microstructure-level finite element-based model for simulation of machining of carbon nanotube reinforced polymer composites," University of Illinois at Urbana-Champaign, 2007.
- [84] R. P. Nimmer and J. T. Woods, "An investigation of brittle failure in ductile, notch-sensitive thermoplastics," *Polymer Engineering & Science*, vol. 32, pp. 1126-1137, 1992.
- [85] H. Nied, V. Stokes, and D. Ysseldyke, "High-Temperature large-strain behavior of polycarbonate, polyetherimide and poly (butylene terephthalate)," *Polymer Engineering & Science*, vol. 27, pp. 101-107, 1987.
- [86] A. Argon and M. Salama, "The mechanism of fracture in glassy materials capable of some inelastic deformation," *Materials Science and Engineering*, vol. 23, pp. 219-230, 1976.
- [87] D. Legrand, "Crazing, yielding, and fracture of polymers. I. Ductile brittle transition in polycarbonate," *Journal of applied polymer science*, vol. 13, pp. 2129-2147, 1969.
- [88] L. Jiang, C. Nath, J. Samuel, and S. G. Kapoor, "An enhanced microstructure-level finite element

- machining model for carbon nanotube-polymer composites," *Journal of Manufacturing Science and Engineering*, vol. 137, 2015.
- [89] F. Müller and J. Monaghan, "Non-conventional machining of particle reinforced metal matrix composite," *International Journal of Machine Tools and Manufacture*, vol. 40, pp. 1351-1366, 2000.
- [90] D. C. Kyritsis, S. Roychoudhury, C. S. McEnally, L. D. Pfefferle, and A. Gomez, "Mesoscale combustion: a first step towards liquid fueled batteries," *Experimental Thermal and Fluid Science*, vol. 28, pp. 763-770, 2004.
- [91] A. Pramanik, L. Zhang, and J. Arsecularatne, "An FEM investigation into the behavior of metal matrix composites: Tool-particle interaction during orthogonal cutting," *International Journal of Machine Tools and Manufacture*, vol. 47, pp. 1497-1506, 2007.
- [92] G. R. Johnson, "A constitutive model and data for metals subjected to large strains, high strain rates and high temperatures," in *Proceedings of the 7th International Symposium on Ballistics, The Hague, Netherlands, 1983*, 1983.
- [93] A. Dwivedi, J. Bradley, and D. Casem, "Mechanical response of polycarbonate with strength model fits," DYNAMIC SCIENCE INC ABERDEEN MD2012.
- [94] J. A. King, D. R. Klimek, I. Miskioglu, and G. M. Odegard, "Mechanical properties of graphene nanoplatelet/epoxy composites," *Journal of Applied Polymer Science*, vol. 128, pp. 4217-4223, 2013.
- [95] W. Tiejun, K. Kishimoto, and M. Notomi, "Effect of triaxial stress constraint on the deformation and fracture of polymers," *Acta Mechanica Sinica*, vol. 18, p. 480, 2002.
- [96] X. Teng, W. Chen, D. Huo, I. Shyha, and C. Lin, "Comparison of cutting mechanism when machining micro and nano-particles reinforced SiC/Al metal matrix composites," *Composite Structures*, vol. 203, pp. 636-647, 2018.
- [97] Z. Yuan, W. Lee, Y. Yao, and M. Zhou, "Effect of crystallographic orientation on cutting forces and surface quality in diamond cutting of single crystal," *CIRP Annals-Manufacturing Technology*, vol. 43, pp. 39-42, 1994.
- [98] M. Malekian, M. Mostofa, S. Park, and M. Jun, "Modeling of minimum uncut chip thickness in micro machining of aluminum," *Journal of Materials Processing Technology*, vol. 212, pp. 553-559, 2012.
- [99] D. Lucca, R. Rhorer, and R. Komanduri, "Energy dissipation in the ultraprecision machining of copper," *CIRP Annals-Manufacturing Technology*, vol. 40, pp. 69-72, 1991.
- [100] A. Dikshit, J. Samuel, R. DeVor, and S. G. Kapoor, "Microstructure-level machining simulation of carbon nanotube reinforced polymer composites—Part II: Model interpretation and application," *Journal of manufacturing science and engineering*, vol. 130, 2008.
- [101] P. Basuray, B. Misra, and G. Lal, "Transition from ploughing to cutting during machining with blunt tools," *Wear*, vol. 43, pp. 341-349, 1977.
- [102] Z. Yuan, M. Zhou, and S. Dong, "Effect of diamond tool sharpness on minimum cutting thickness and cutting surface integrity in ultraprecision machining," *Journal of Materials Processing Technology*, vol. 62, pp. 327-330, 1996.
- [103] S. Shimada, N. Ikawa, H. Tanaka, G. Ohmori, J. Uchikoshi, and H. Yoshinaga, "Feasibility study on ultimate accuracy in microcutting using molecular dynamics simulation," *CIRP Annals-Manufacturing Technology*, vol. 42, pp. 91-94, 1993.
- [104] S. Filiz, C. M. Conley, M. B. Wasserman, and O. B. Ozdoganlar, "An experimental investigation of micro-machinability of copper 101 using tungsten carbide micro-endmills," *International Journal of Machine Tools and Manufacture*, vol. 47, pp. 1088-1100, 2007.
- [105] K. Kwang-Ryul, C. Byoung-Deog, Y. Jun-Sin, C. Sung-Hak, C. Yong-Ho, S. Dong-Soo, *et al.*, "Laser micromachining of CNT/Fe/Al₂O₃ nanocomposites," *Transactions of Nonferrous Metals Society of China*, vol. 19, pp. s189-s193, 2009.
- [106] Y. Wan, D. Kim, Y.-B. Park, and S.-K. Joo, "Micro electro discharge machining of polymethylmethacrylate (PMMA)/multi-walled carbon nanotube (MWCNT) nanocomposites," *Advanced Composites Letters*, vol. 17, p. 096369350801700401, 2008.

Figure Captions List

Figure 1 The development of achievable machining accuracy (Reprinted from

Fig. 1 [2]The development of achievable machining accuracy (Reprinted from
[2] Copyright 2003, with permission from CIRP)

Formatted: F
grammar

Formatted: F
grammar

Figure 2 Size effects in micro-milling metals and alloys (Reproduced from [14-

Fig. 2 16])Size effects in micro-milling metals and alloys (Reproduced from [14-
16])

Formatted: F
grammar

Figure 3 Size effect on specific cutting energy in micro-milling as compared to

Fig. 3 macro-machining (Reproduced from [15]Size effect on specific cutting
energy in micro-milling as compared to macro-machining (Reproduced
from [15])

Formatted: F
grammar

Formatted: F

Figure 4 The schematic representing the differences between macro and

Fig. 4 micromachining in terms of microstructure (Reprinted from [97]
Copyright 1994, with permission from CIRP)The schematic representing
the differences between macro and micromachining in terms of
microstructure (Reprinted from [97] Copyright 1994, with permission
from CIRP)

Formatted: F
grammar

Formatted: F

Figure 5 Effect of microstructure on surface quality when micro-milling steel

Fig. 5 (Reproduced from [24]Effect of microstructure on surface quality when
micro-milling steel (Reproduced from [24])

Formatted: F
grammar

Formatted: F
grammar

Formatted: F

Figure 6 Grain size effect on surface roughness and hardness when micromachining W/Cu composite (Reproduced from [27])
~~Fig. 6 Grain size effect on surface roughness and hardness when micromachining W/Cu composite (Reproduced from [27])~~

Formatted: F
grammar

Figure 7 Tool edge radius and feed-rate effects on surface roughness in micro-milling (Reproduced from [16, 26])
~~Fig. 7 Tool edge radius and feed-rate effects on surface roughness in micro-milling (Reproduced from [16, 26])~~

Formatted: F
grammar

Figure 8 MUCT effects on the cutting mechanism in micromachining (Reprinted from [98] Copyright 2011, with permission from Elsevier)
~~Fig. 8 MUCT effects on the cutting mechanism in micromachining (Reprinted from [98] Copyright 2011, with permission from Elsevier)~~

Formatted: F
grammar

Figure 9 Effects of MUCT on the shear angle of materials in micromachining (Reprinted from [99] Copyright 1991, with permission from CIRP)
~~Fig. 9 Effects of MUCT on the shear angle of materials in micromachining (Reprinted from [99] Copyright 1991, with permission from CIRP)~~

Formatted: F
grammar

Figure 10 Various surface roughness with different nano-fillers and feed rate in micro-milling PC-based nanocomposites (Reproduced from [46])
~~Fig. 10 Various surface roughness with different nano-fillers and feed rate in micro-milling PC-based nanocomposites (Reproduced from [46])~~

Formatted: F
grammar

Figure 11 Effect of CNT addition on chip formation of PC/MWCNT nanocomposite (Reprinted with permission from [45]. Copyright 2006 by ASME)
~~Fig. 11 CNT addition on chip formation of PC/MWCNT nanocomposite (Reprinted with permission from [45]. Copyright 2006 by ASME)~~

Formatted: F
grammar

Figure 12 Comparison of surface roughness when micro-milling PC/ 15 wt.%

Fig. 12 MWCNT nanocomposite and plain PC (Reproduced from

[45])

Comparison of surface roughness when micro-milling PC/ 15 wt.% MWCNT nanocomposite and plain PC (Reproduced from [45])

Formatted: F grammar

Figure 13 Comparison of the resultant cutting forces for plain PC and PC/CNT

Fig. 13 nanocomposites (Adapted from [45, 51])

Comparison of the resultant cutting forces for plain PC and PC/CNT nanocomposites (Adapted from

{45, 51})

Formatted: F grammar

Formatted: B

Figure 14 Effect of CNT orientation on cutting force when micro-milling PC/5 wt.%

Fig. 14 MWCNT nanocomposites (Reproduced from [51])

Effect of CNT orientation on cutting force when micro-milling PC/5 wt.% MWCNT

nanocomposites (Reproduced from [51])

Formatted: F grammar

Figure 15 Effects of CNT loading and feed rate on surface roughness and burr width

Fig. 15 when micro-milling PC/MWCNT nanocomposites at cutting speed = 130

m/min (Reproduced from [44])

Effects of CNT loading and feed rate on surface roughness and burr width when micro-milling PC/MWCNT

nanocomposites at cutting speed = 130 m/min (Reproduced from [44])

Formatted: F grammar

Figure 16 Effects of MUCT (feed rate), cutting speed (strain rate) and CNT loading

Fig. 16 on cutting force when micro-milling PC/MWCNT nanocomposites

(Reproduced from [44])

Effects of MUCT (feed rate), cutting speed (strain rate) and CNT loading on cutting force when micro-milling PC/MWCNT

nanocomposites (Reproduced from [44])

Figure 17 Schematic of micro-milling CNT-based nanocomposite (Reprinted with permission from [51] . Copyright 2013 by ASME)
~~17 Fig. Schematic of micro-milling CNT-based nanocomposite (Reprinted with permission from [51] . Copyright 2013 by ASME)~~

Formatted: F
grammar

Formatted: F
grammar

Formatted: F

Figure 18 Influence of the matrix-fiber bond's strength to the chip formation and surface generation (Reprinted with permission from [49]. Copyright 2015 by ASME)
~~18 Fig. Influence of the matrix-fiber bond's strength to the chip formation and surface generation (Reprinted with permission from [49]. Copyright 2015 by ASME)~~

Formatted: F
grammar

Figure 19 Effect of cutting speed on cutting force and surface roughness when micromachining epoxy/0.8 vol.% GF and epoxy/0.8 vol.% GF/0.2 wt.% GPL composites (Reproduced from [49])
~~19 Fig. Effect of cutting speed on cutting force and surface roughness when micromachining epoxy/0.8 vol.% GF and epoxy/0.8 vol.% GF/0.2 wt.% GPL composites (Reproduced from [49])~~

Formatted: F
grammar

Figure 20 Effect of cutting speed and filler content on cutting force when micro-milling different polymer nanocomposites at feed rate = 3 $\mu\text{m}/\text{tooth}$ (Reproduced from [44, 54])
~~20 Fig. Effect of cutting speed and filler content on cutting force when micro-milling different polymer nanocomposites at feed rate = 3 $\mu\text{m}/\text{tooth}$ (Reproduced from [44, 54])~~

Figure 21 Different trends of cutting forces as a function of graphene addition when micromachining graphene reinforced PMNCs (Reproduced from [49, 54, 56])
~~21 Fig. Different trends of cutting forces as a function of graphene~~

~~addition when micromachining graphene reinforced PMNCs~~

~~(Reproduced from [49, 54, 56])~~

Figure Quantitative comparison of the standardized effects of various

22—Fig. parameters on cutting forces for Mg/Graphene nanocomposites

22 ~~(Reproduced from [57])Quantitative comparison of the standardized~~

~~effects of various parameters on cutting forces for Mg/Graphene~~

~~nanocomposites (Reproduced from [57])~~

Formatted: F
grammar

Formatted: D

Formatted: F
grammar

Figure Specific cutting energy when micro-milling Mg and Mg/10 vol.% SiC

23—Fig. nanocomposite (Reproduced from [58])Specific cutting energy when

23 ~~micro-milling Mg and Mg/10 vol.% SiC nanocomposite (Reproduced from~~

~~[58])~~

Formatted: F
grammar

Figure Effect of SiC content on cutting force when micro-milling Mg/SiC

24—Fig. nanocomposite (Reproduced from [59])Effect of SiC content on cutting

24 ~~force when micro-milling Mg/SiC nanocomposite (Reproduced from~~

~~[59])~~

Formatted: F
grammar

Figure Effect of feed rate on cutting force when micromachining Mg/ceramic

25—Fig. nanocomposites (Adapted from [59, 60])Effect of feed rate on cutting

25 ~~force when micromachining Mg/ceramic nanocomposites (Adapted~~

~~from [59, 60])~~

Formatted: F
grammar

Figure Schematic showing the correlations between micro-machinability of

26—Fig. nanocomposites and some basic factors

26

Formatted: F
grammar

Figure 27 Micro-structure-level machining of CNT reinforced polycarbonate

Fig. 27 (Reprinted with permission from [100]. Copyright 2008 by ASME)
Micro-structure-level machining of CNT reinforced polycarbonate (Reprinted with permission from [100]. Copyright 2008 by ASME)

Formatted: F
grammar

Formatted: C
border)

Figure 28 Micro-structure-level machining of CNT reinforced PVA nanocomposite

Fig. 28 (Reprinted with permission from [88]. Copyright 2014 by ASME)
Micro-structure-level machining of CNT reinforced PVA nanocomposite (Reprinted with permission from [88]. Copyright 2014 by ASME)

Formatted: F
grammar

Formatted: F

Formatted: F

Formatted: F

Figure 29 Finite element analysis of micro-milling PC and PC reinforced GNP

Fig. 29 nanocomposite: (a) Chip formation of PC/GNP, (b) Cutting forces in simulation and experiment (Reprinted from [46] Copyright 2017, with permission from Elsevier)
Finite element analysis of micro-milling PC and PC reinforced GNP nanocomposite: (a) Chip formation of PC/GNP, (b) Cutting forces in simulation and experiment (Reprinted from [46] Copyright 2017, with permission from Elsevier)

Formatted: F
grammar

Figure 30 Finite element analysis of micro-milling Mg reinforced by 1.5 vol.% SiC

Fig. 30 nanocomposite (Reprinted from [71] Copyright 2018, with permission from The Society of Manufacturing Engineers)
Finite element analysis of micro-milling Mg reinforced by 1.5 vol.% SiC nanocomposite (Reprinted from [71] Copyright 2018, with permission from The Society of Manufacturing Engineers)

Formatted: F
grammar

Figure Effect of nano-particles on shear zone propagation: (a) direction of shear
31Fig. zone propagation, (b) distorted stress contour caused by particle
31 restricting behavior (Reprinted from [96] Copyright 2018, with
permission from Elsevie)Effect of nano-particles on shear zone
propagation: (a) direction of shear zone propagation, (b) distorted stress
contour caused by particle restricting behavior (Reprinted from [96]
Copyright 2018, with permission from Elsevie)

Formatted: F
grammar

Table Caption List

<u>Table</u>	<u>The MUCT effects in micromachining – Relevant researches</u>
<u>1Table-1</u>	<u>MUCT effects in micromachining – Relevant researches</u>
<u>Table</u>	<u>Summary of micromachining CNT reinforced polymer matrix</u>
<u>2Table-2</u>	<u>nanocomposites</u> <u>Summary of micromachining CNT reinforced</u> <u>polymer matrix nanocomposites</u>
<u>Table</u>	<u>Summary of micromachining graphene reinforced polymer matrix</u>
<u>3Table-3</u>	<u>nanocomposites</u> <u>Summary of micromachining graphene reinforced</u> <u>polymer matrix nanocomposites</u>
<u>Table</u>	<u>Summary of micromachining nano-ceramic-particles reinforced</u>
<u>4Table-4</u>	<u>metal matrix nanocomposites</u> <u>Summary of micromachining nano-</u> <u>ceramic-particles reinforced metal matrix nanocomposites</u>
<u>Table</u>	<u>Summary of micromachining of nanocomposites employing other</u>
<u>5Table-5</u>	<u>micro-fabrication techniques</u> <u>Summary of micromachining of</u> <u>nanocomposites employing other micro-fabrication techniques</u>

Formatted: F

Formatted: F

Formatted: B

Formatted: F

Formatted: F

Information Regarding Figures and Tables

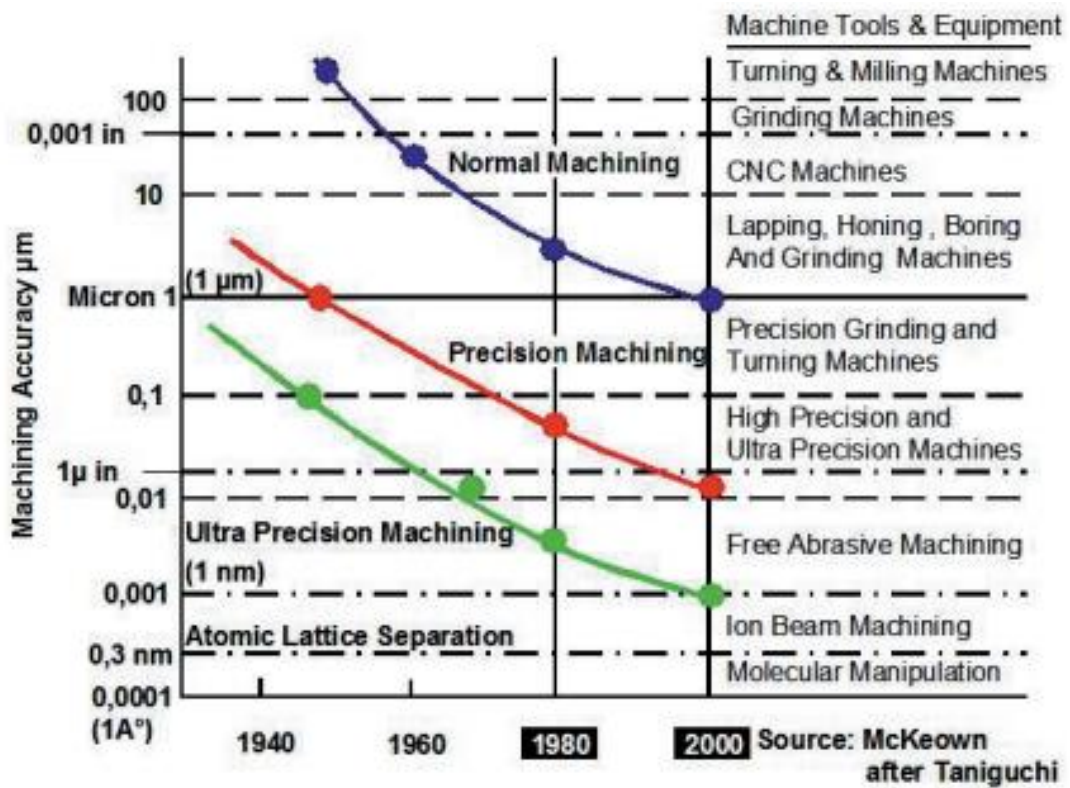


Figure 1: The development of achievable machining accuracy (Reprinted from [2])

Copyright 2003, with permission from CIRP)

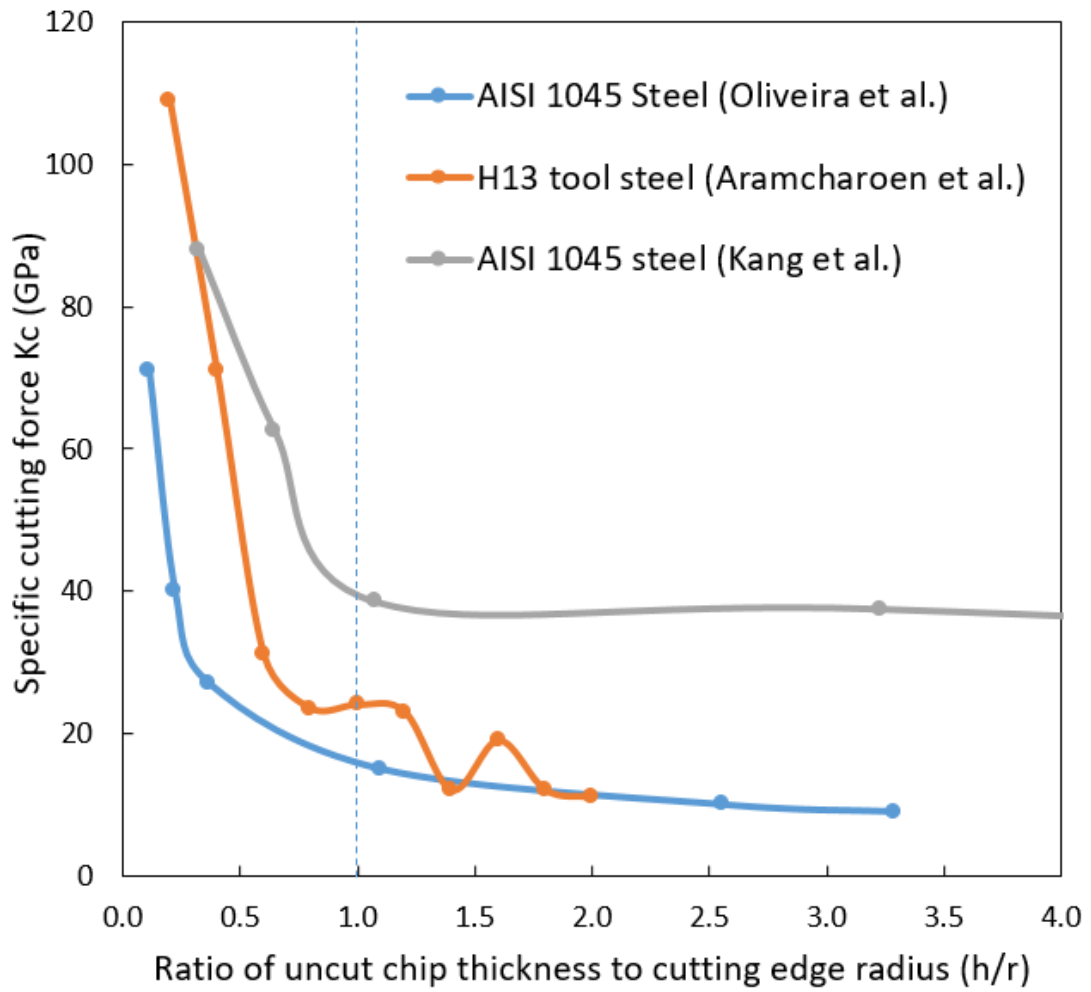


Figure 2: Size effects in micro-milling metals and alloys (Reproduced from [14-16])

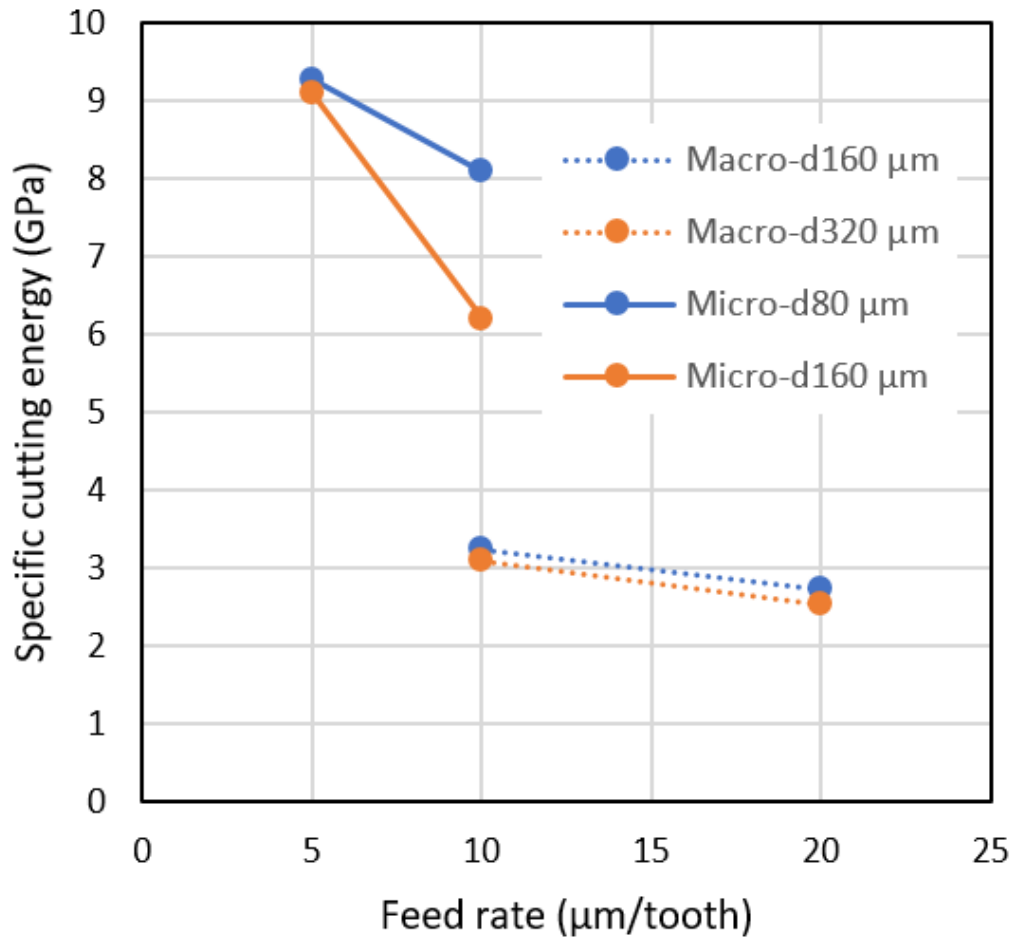


Figure 3: Size effect on specific cutting energy in micro-milling as compared to macro-machining (Reproduced from [15])

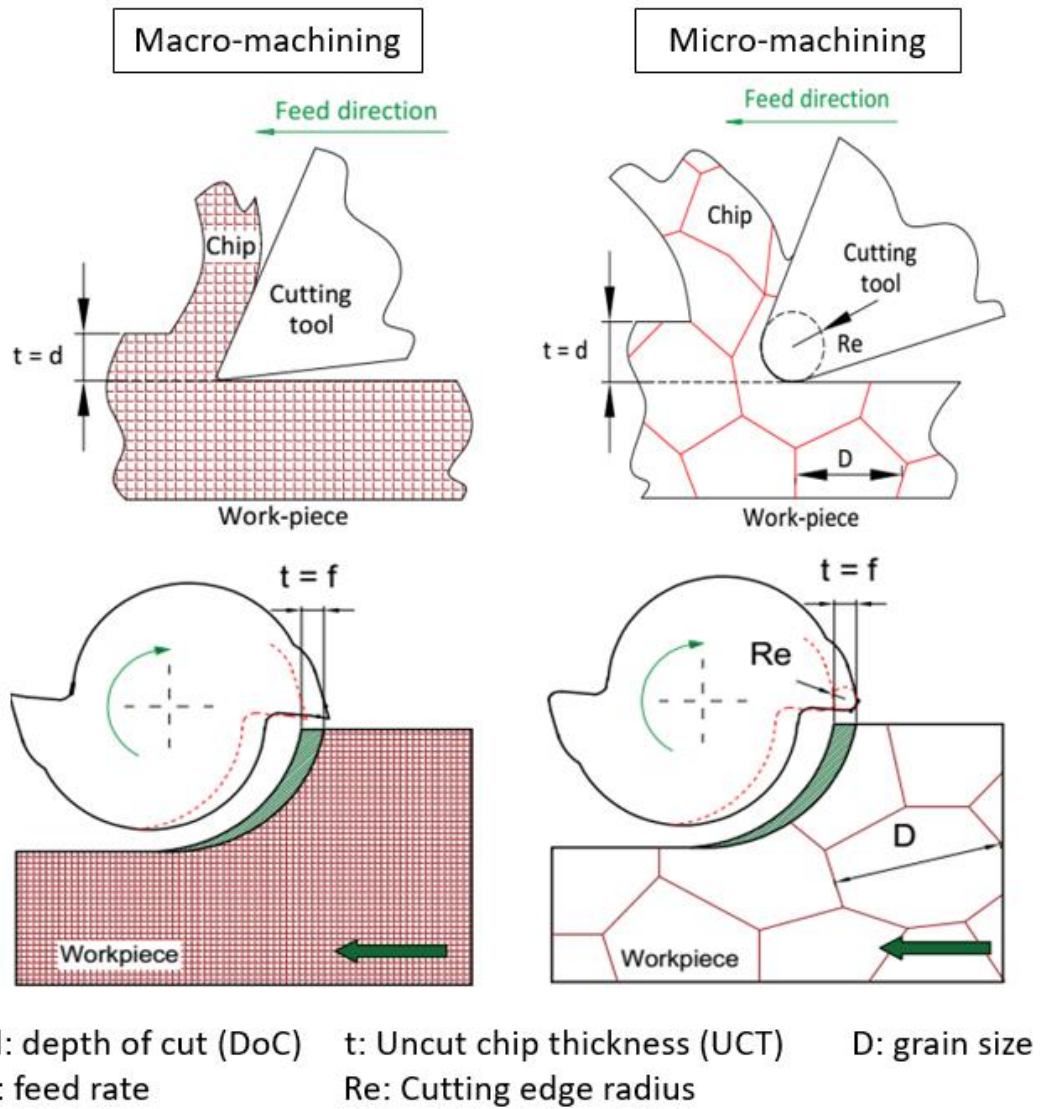


Figure 4: The schematic representing the differences between macro and micromachining in terms of microstructure (Reprinted from [97] Copyright 1994, with permission from CIRP)

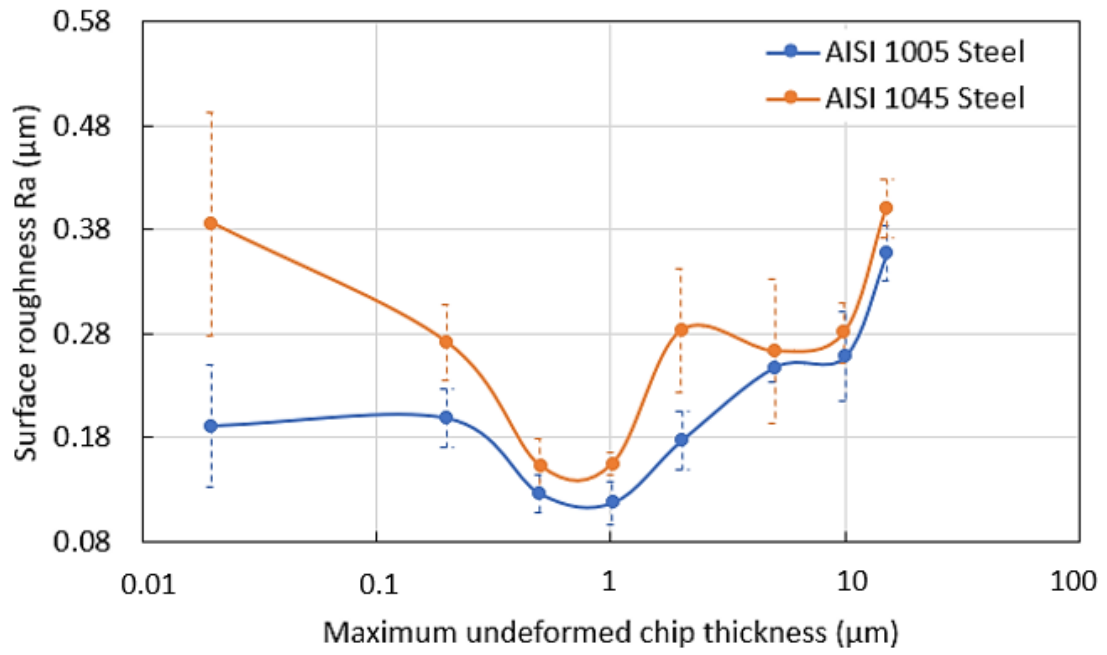


Figure 5: Effect of microstructure on surface quality when micro-milling steel

(Reproduced from [24])

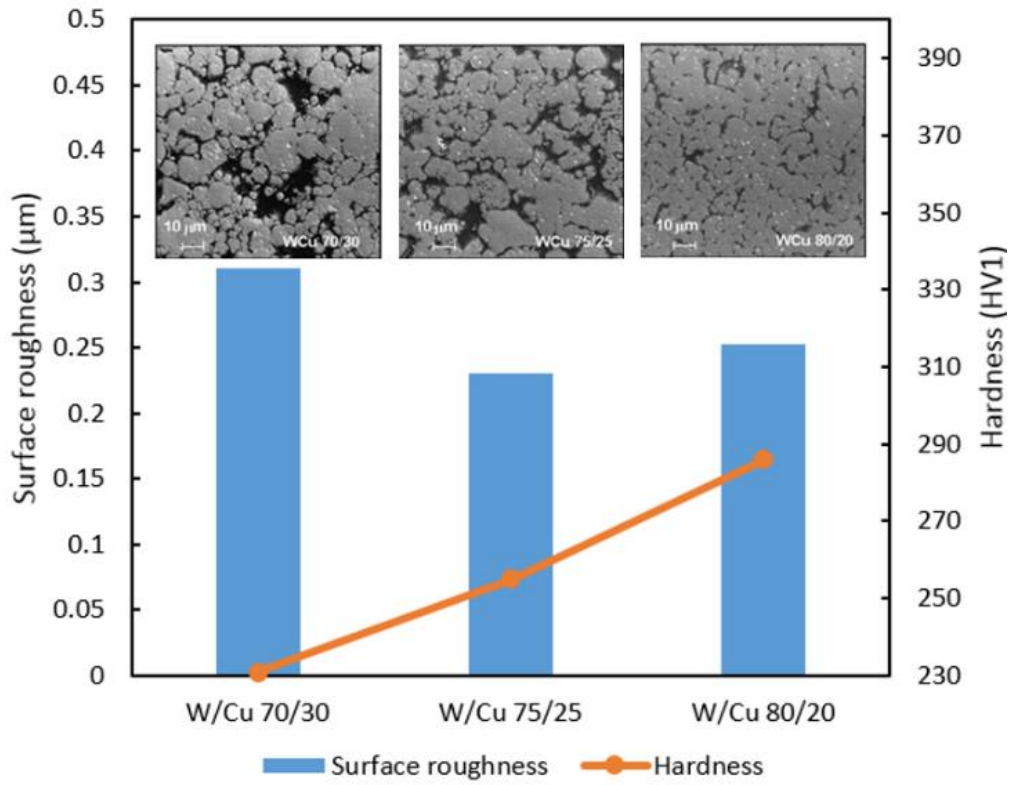


Figure 6: Grain size effect on surface roughness and hardness when micromachining W/Cu composite (Reproduced from [27])

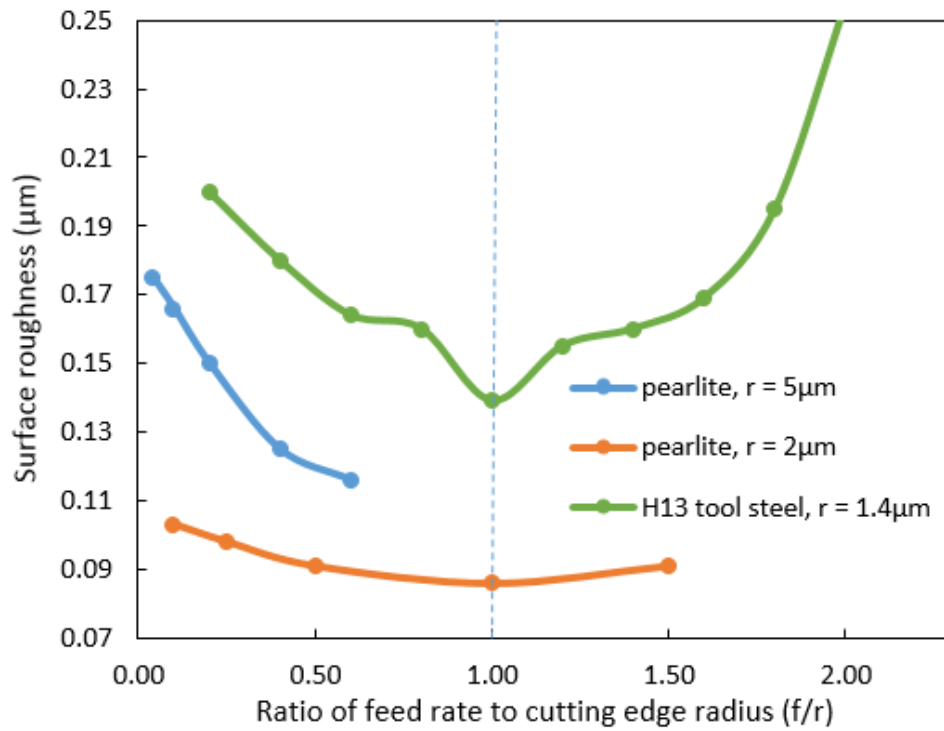


Figure 7: Tool edge radius and feed-rate effects on surface roughness in micro-milling

(Reproduced from [16, 26])

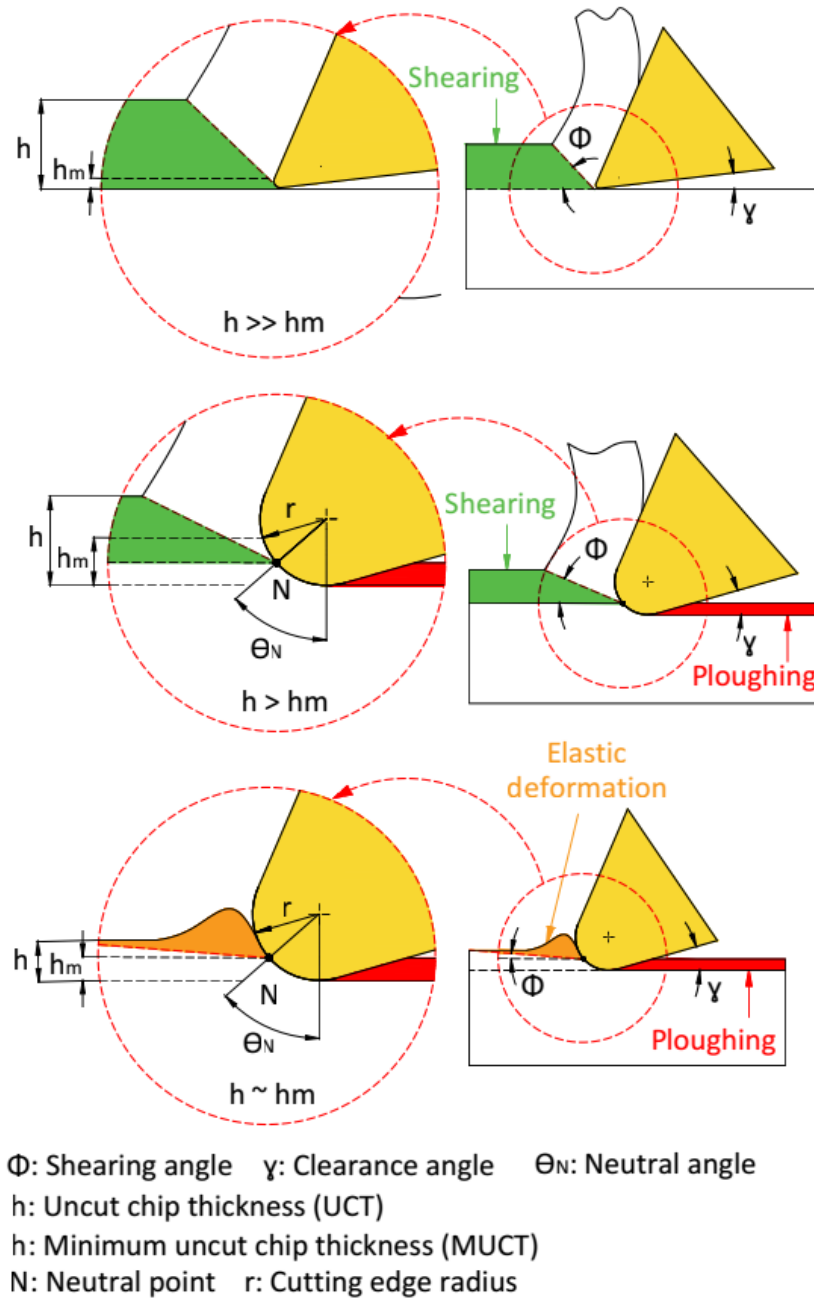


Figure 8: MUCT effects on the cutting mechanism in micromachining (Reprinted from [98] Copyright 2011, with permission from Elsevier)

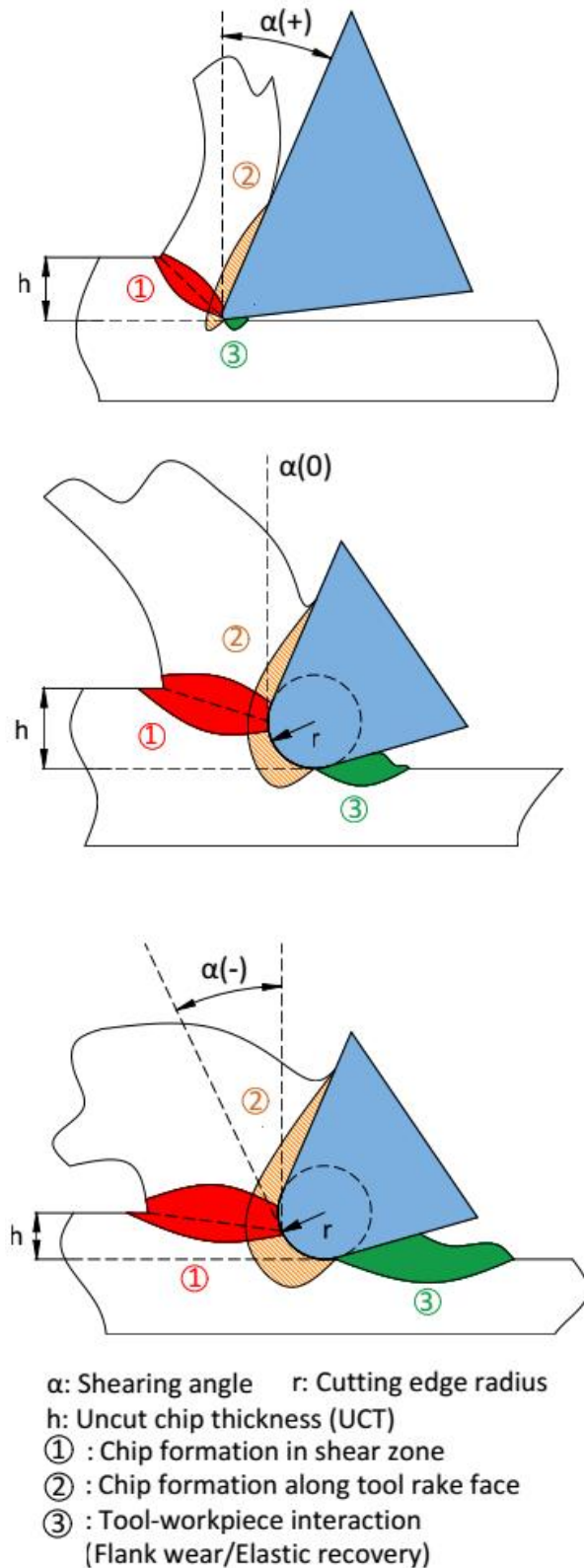


Figure 9: Effects of MUCT on the shear angle of materials in micromachining (Reprinted from [99] Copyright 1991, with permission from CIRP)

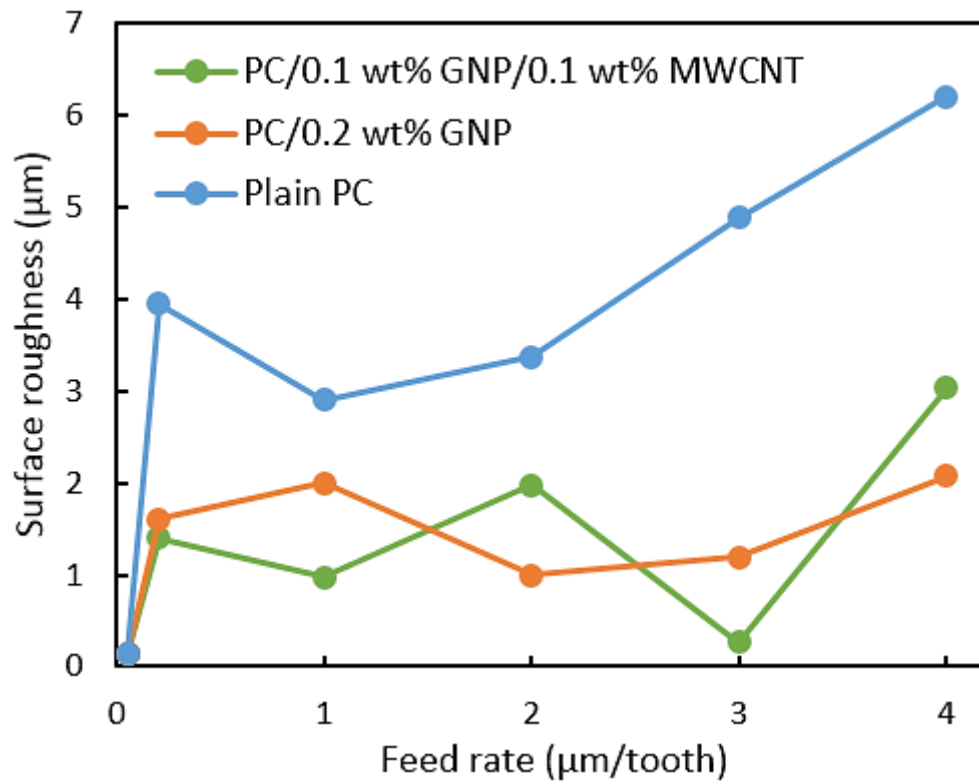


Figure 10: Various surface roughness with different nano-fillers and feed rate in micro-milling PC-based nanocomposites (Reproduced from [46])

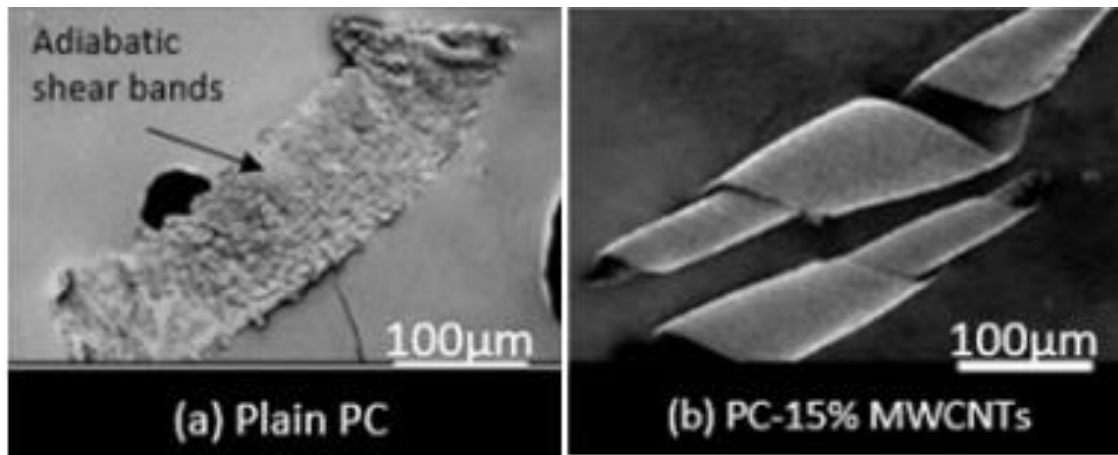


Figure 11: Effect of CNT addition on chip formation of PC/MWCNT nanocomposite
(Reprinted with permission from [45]. Copyright 2006 by ASME)

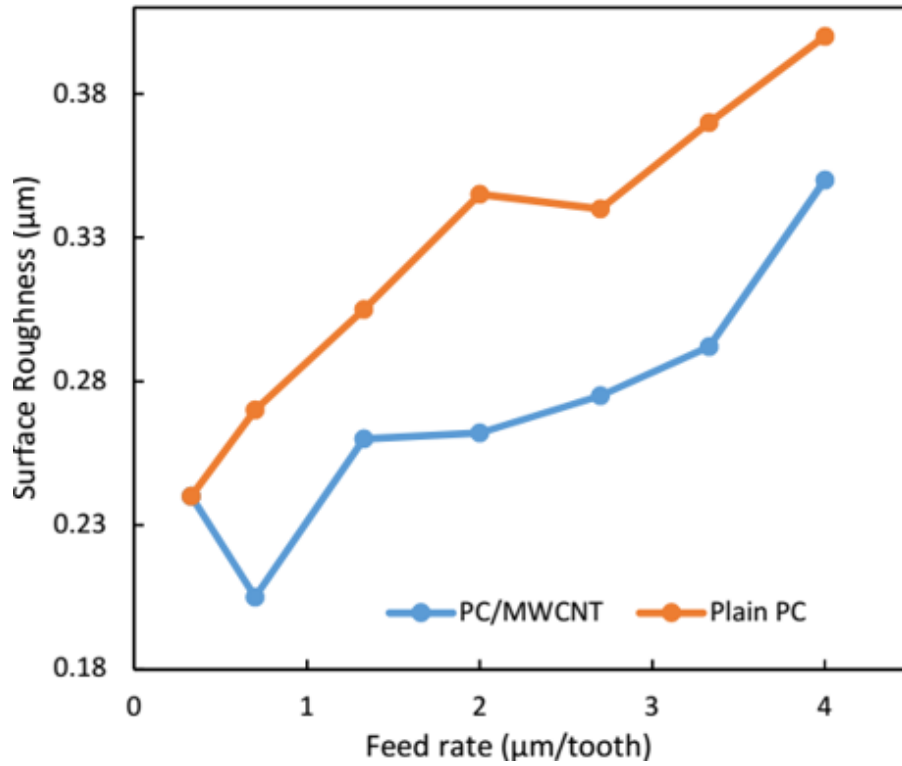


Figure 12: Comparison of surface roughness when micro-milling PC/ 15 wt.% MWCNT nanocomposite and plain PC (Reproduced from [45])

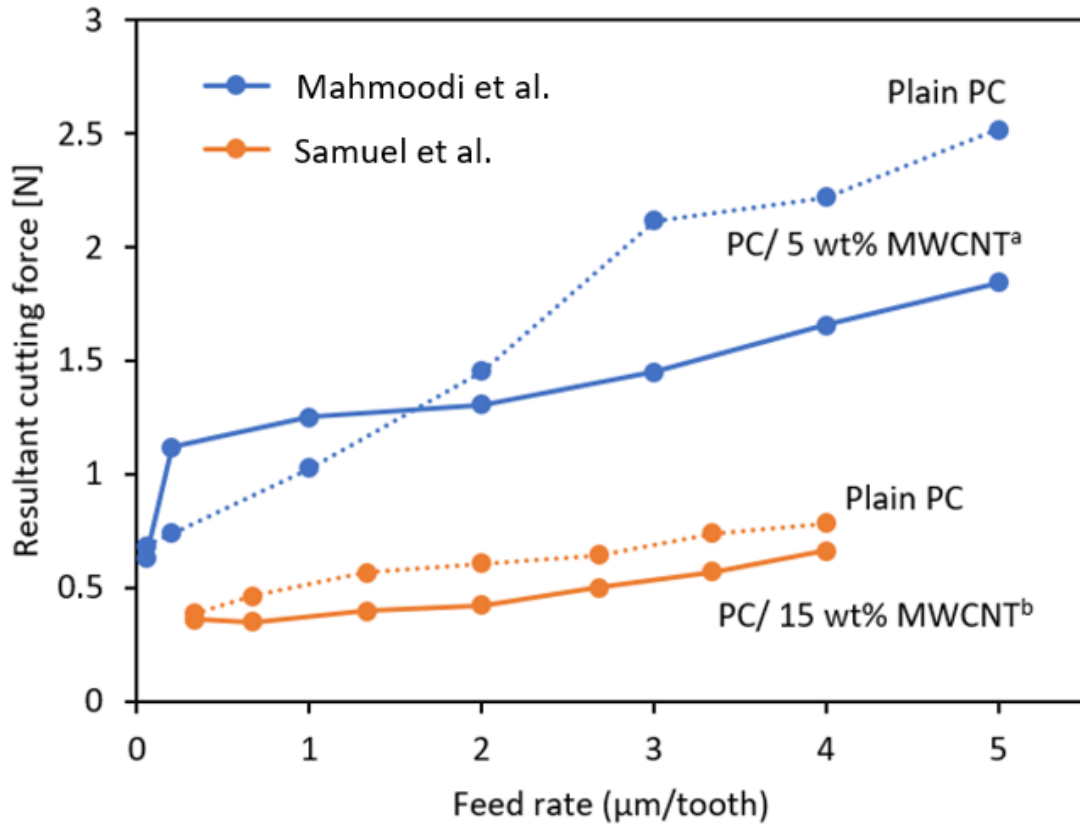


Figure 13: Comparison of the resultant cutting forces for plain PC and PC/CNT nanocomposites (Adapted from [45, 51])

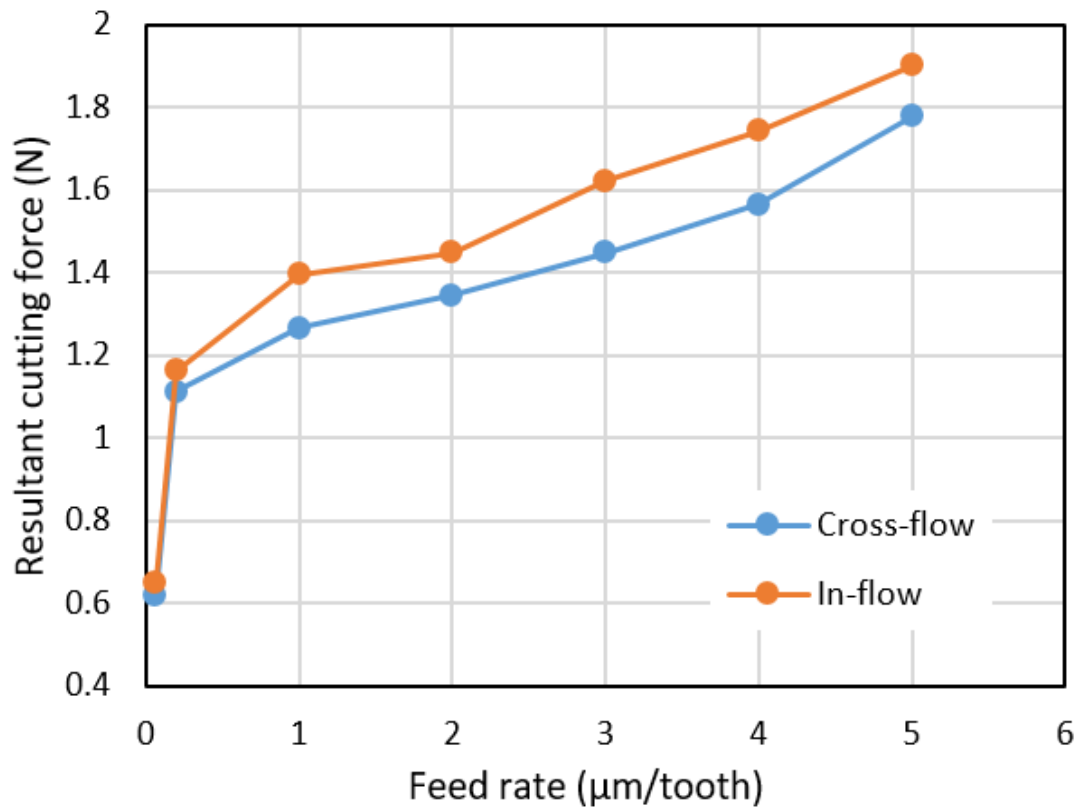


Figure 14: Effect of CNT orientation on cutting force when micro-milling PC/5 wt.% MWCNT nanocomposites (Reproduced from [51])

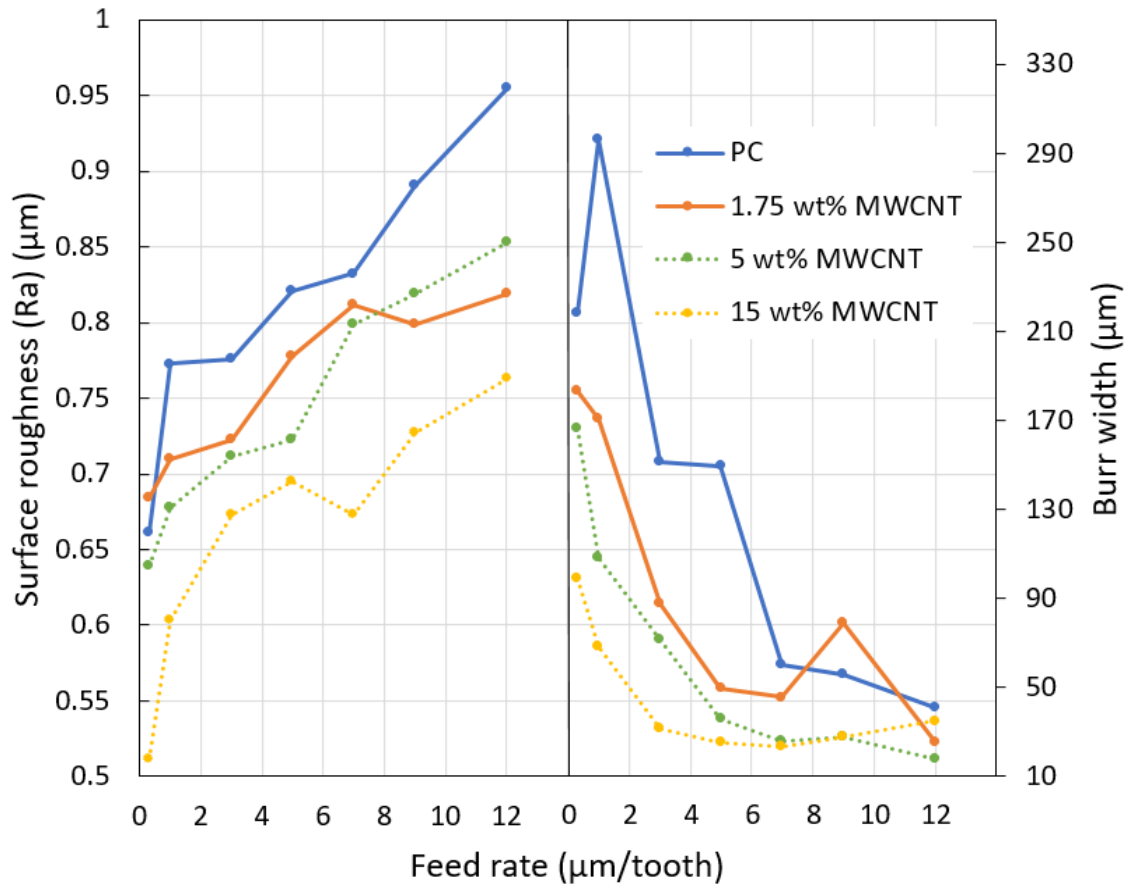


Figure 15: Effects of CNT loading and feed rate on surface roughness and burr width when micro-milling PC/MWCNT nanocomposites at cutting speed = 130 m/min (Reproduced from [44])

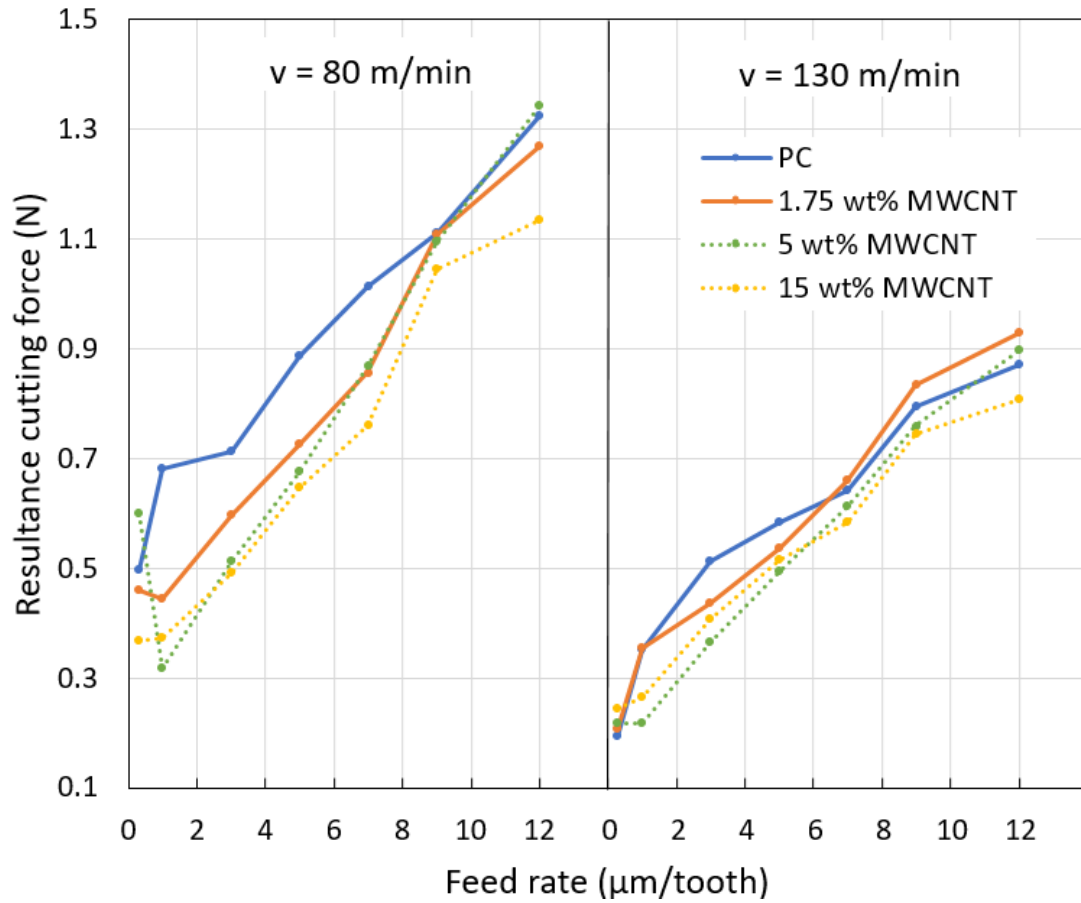


Figure 16: Effects of MUCT (feed rate), cutting speed (strain rate) and CNT loading on cutting force when micro-milling PC/MWCNT nanocomposites (Reproduced from [44])

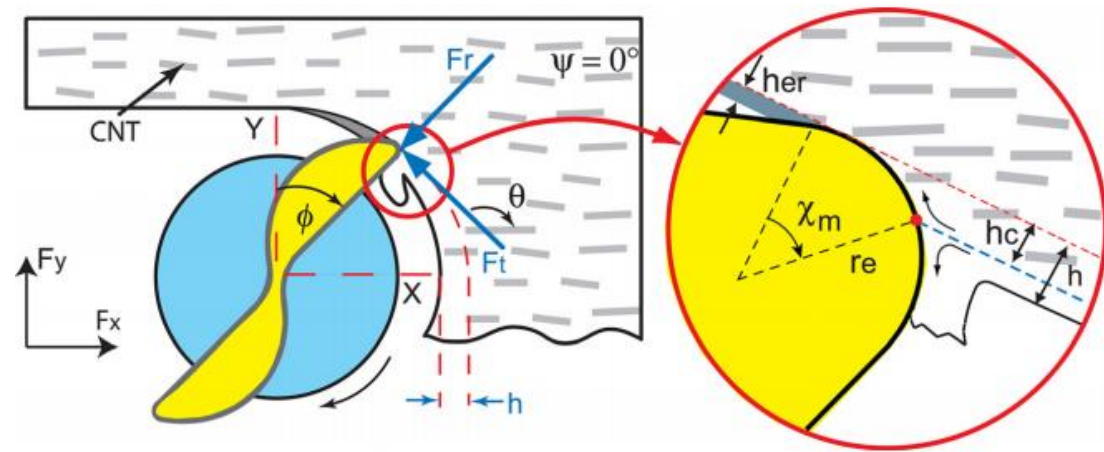


Figure 17: Schematic of micro-milling CNT-based nanocomposite (Reprinted with permission from [51] . Copyright 2013 by ASME)

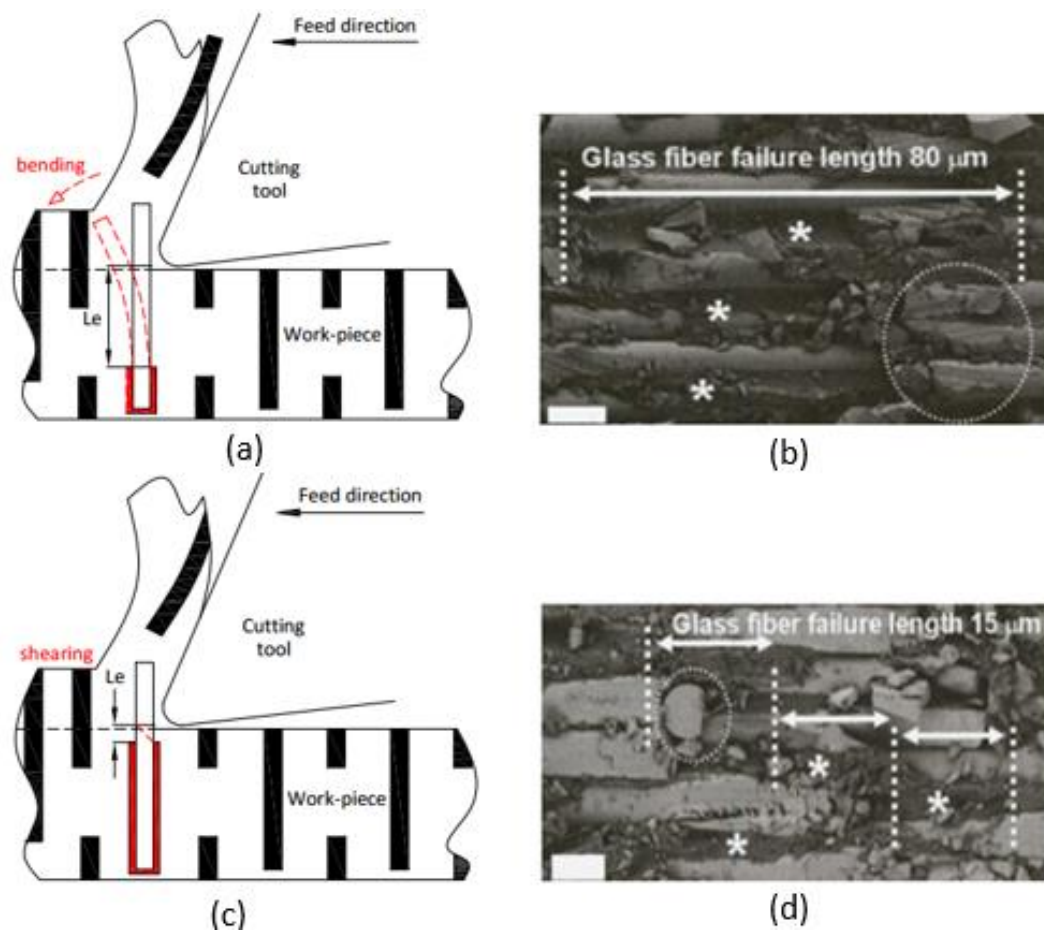


Figure 18: Influence of the matrix-fiber bond's strength to the chip formation and surface generation (Reprinted with permission from [49]. Copyright 2015 by ASME)

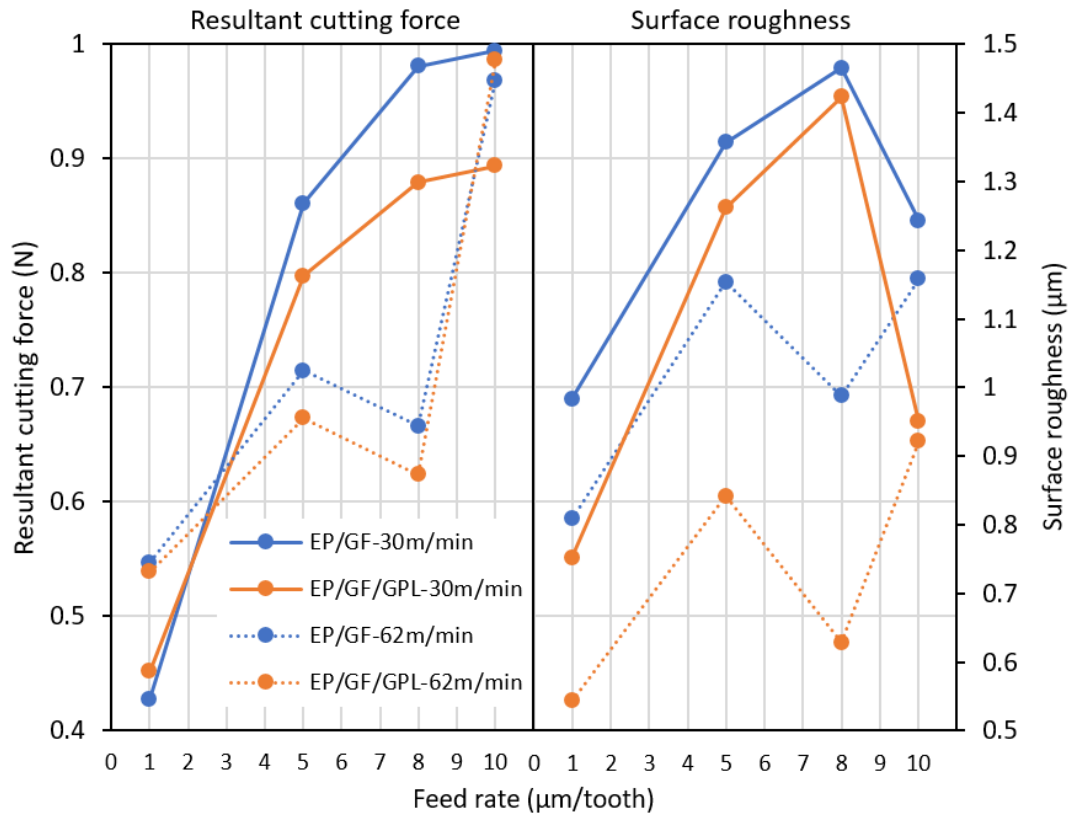


Figure 19: Effect of cutting speed on cutting force and surface roughness when micromachining epoxy/0.8 vol.% GF and epoxy/0.8 vol.% GF/0.2 wt.% GPL composites (Reproduced from [49])

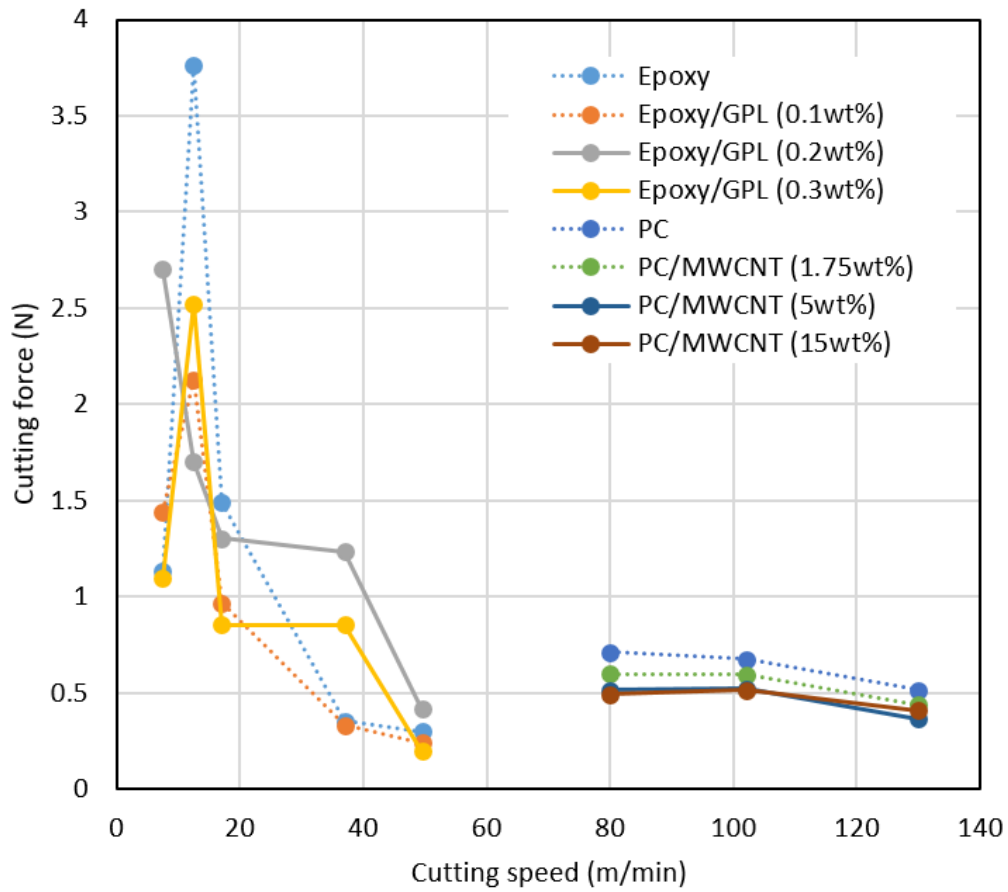


Figure 20: Effect of cutting speed and filler content on cutting force when micro-milling different polymer nanocomposites at feed rate = 3 $\mu\text{m}/\text{tooth}$ (Reproduced from [44, 54])

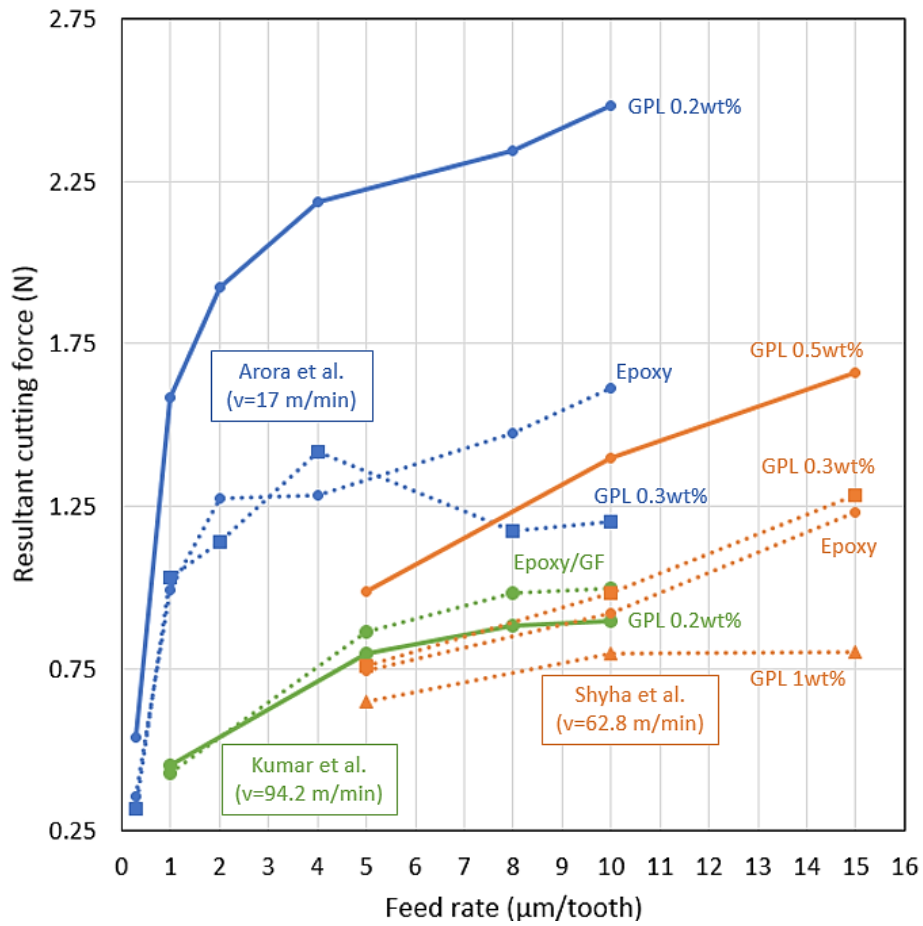


Figure 21: Different trends of cutting forces as a function of graphene addition when micromachining graphene reinforced PMNCs (Reproduced from [49, 54, 56])

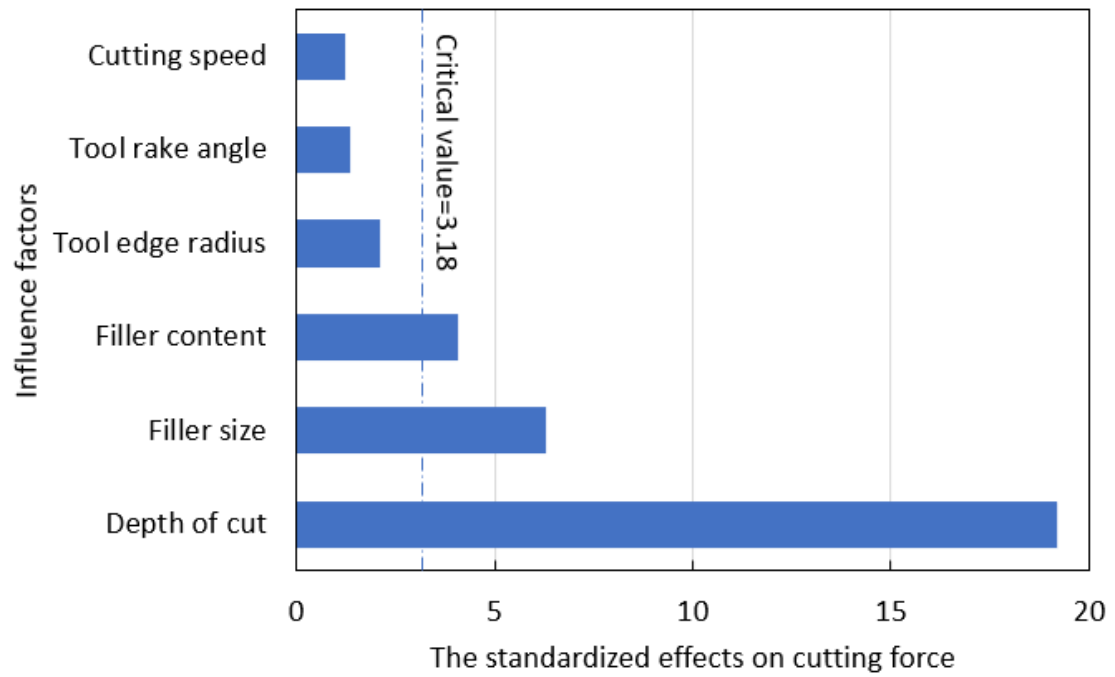


Figure 22: Quantitative comparison of the standardized effects of various parameters on cutting forces for Mg/Graphene nanocomposites (Reproduced from [57])

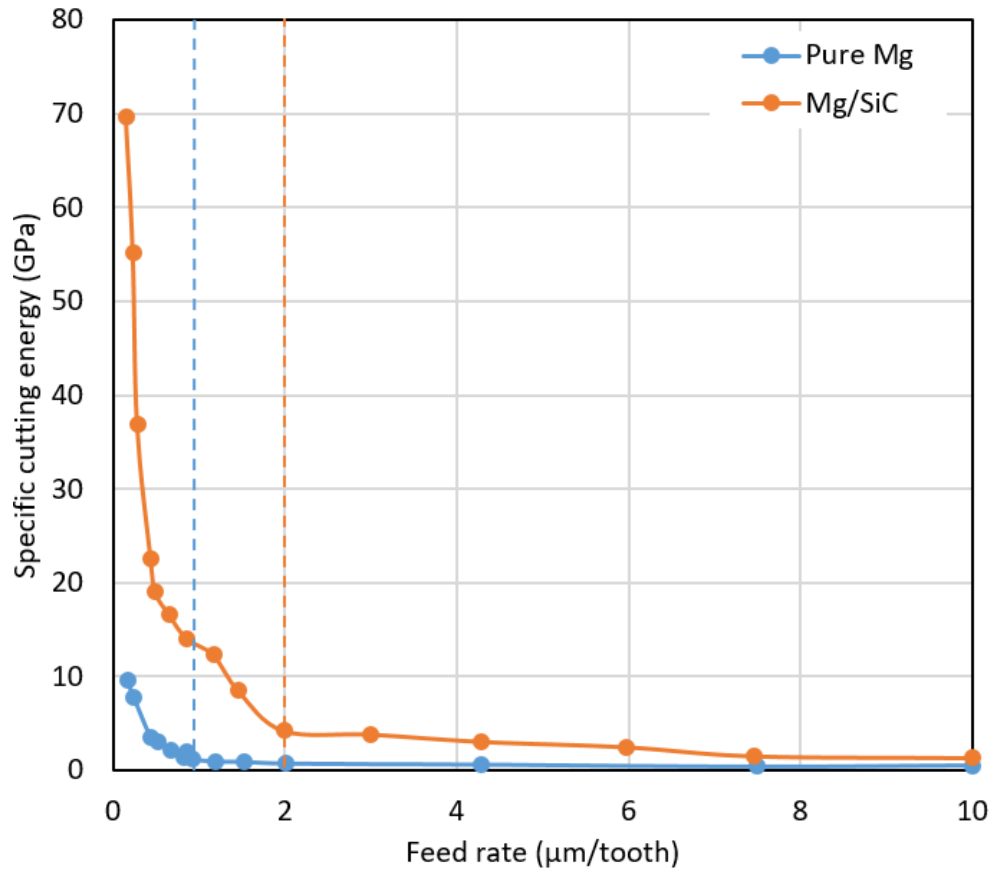


Figure 23: Specific cutting energy when micro-milling Mg and Mg/10 vol.% SiC nanocomposite (Reproduced from [58])

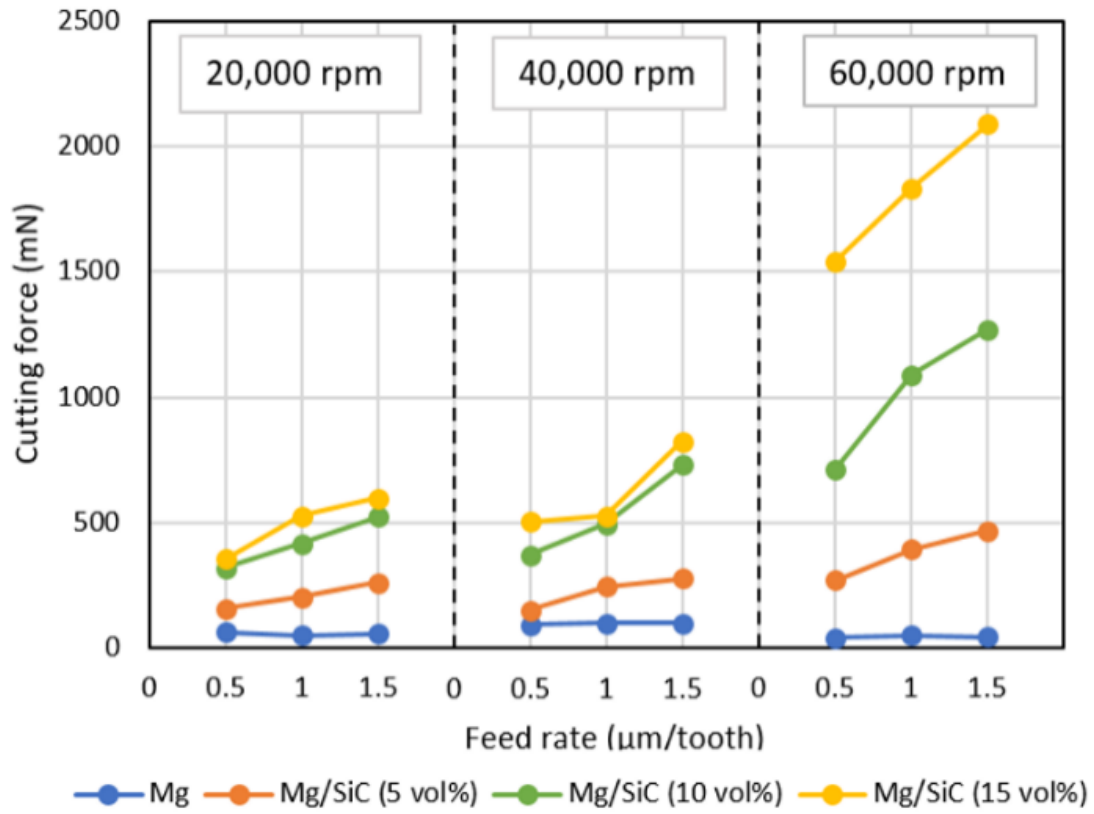


Figure 24: Effect of SiC content on cutting force when micro-milling Mg/SiC nanocomposite (Reproduced from [59])

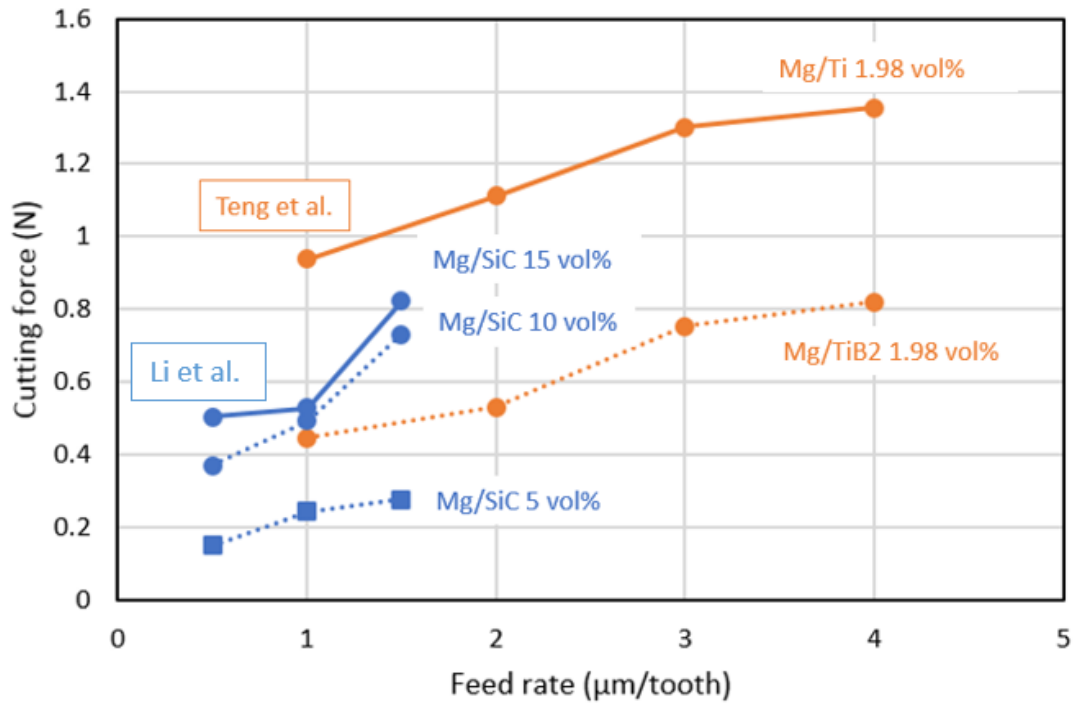


Figure 25: Effect of feed rate on cutting force when micromachining Mg/ceramic nanocomposites (Adapted from [59, 60])

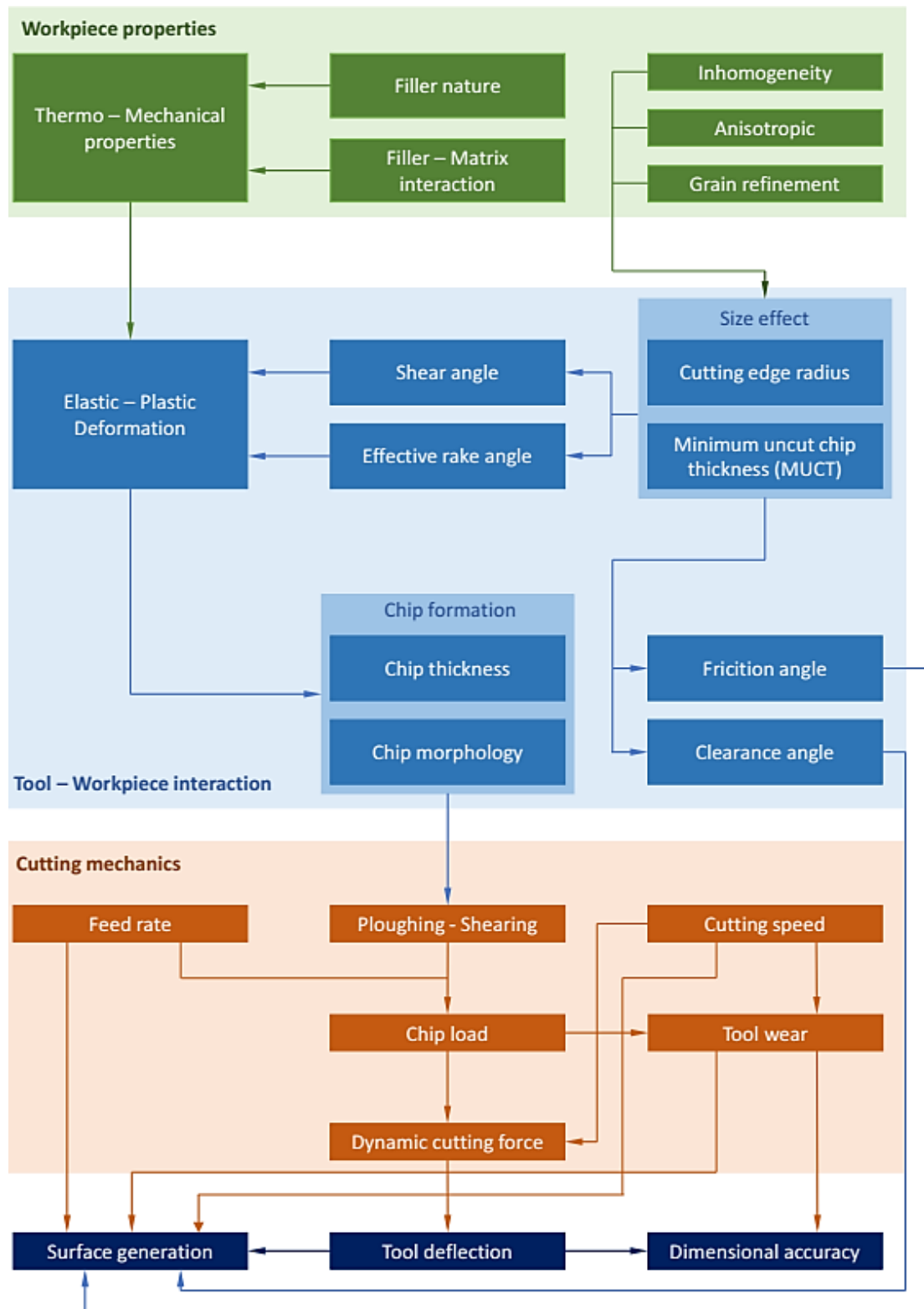


Figure 26: Schematic showing the correlations between micro-machinability of nanocomposites and some basic factors

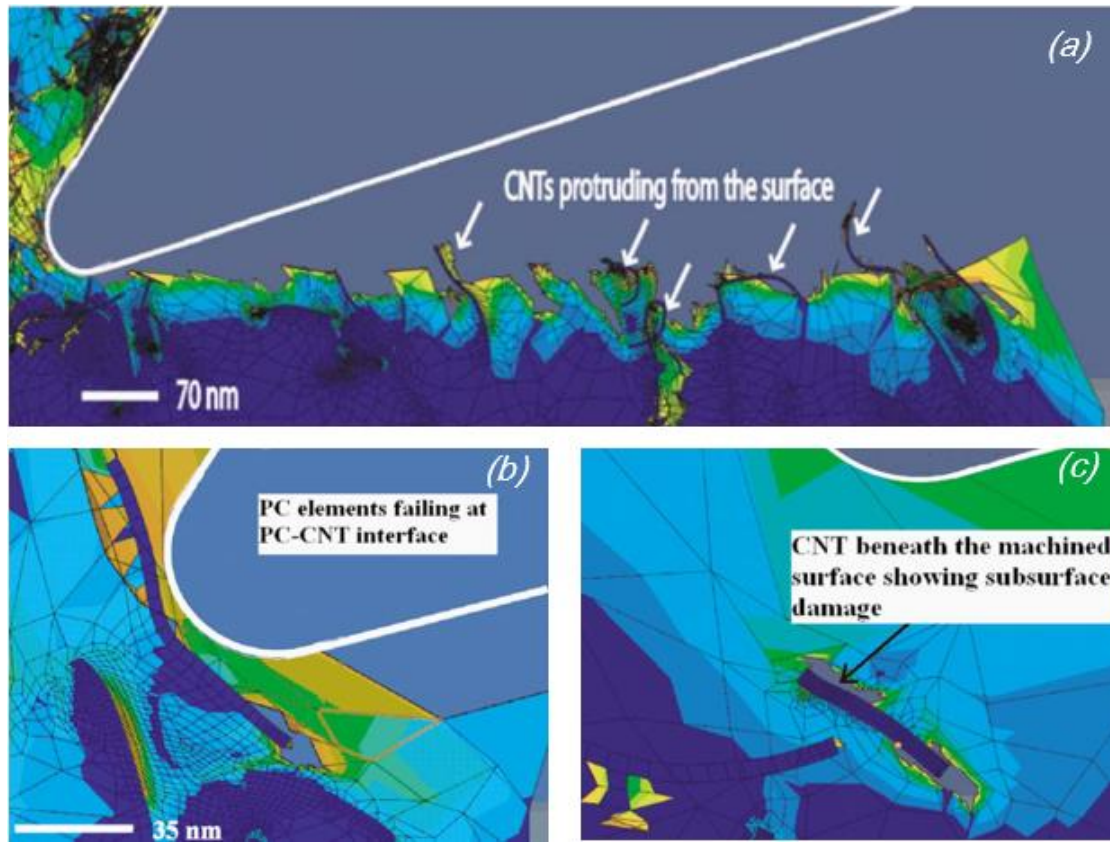


Figure 27: Micro-structure-level machining of CNT reinforced polycarbonate
(Reprinted with permission from [100] Copyright 2008 by ASME)

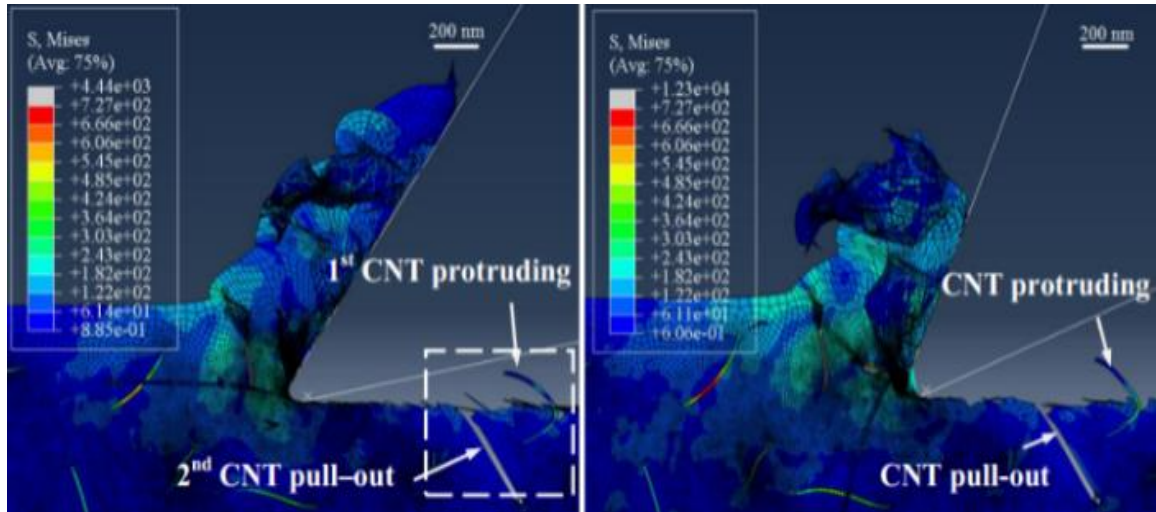


Figure 28: Micro-structure-level machining of CNT reinforced PVA nanocomposite

(Reprinted with permission from [88] . Copyright 2014 by ASME)

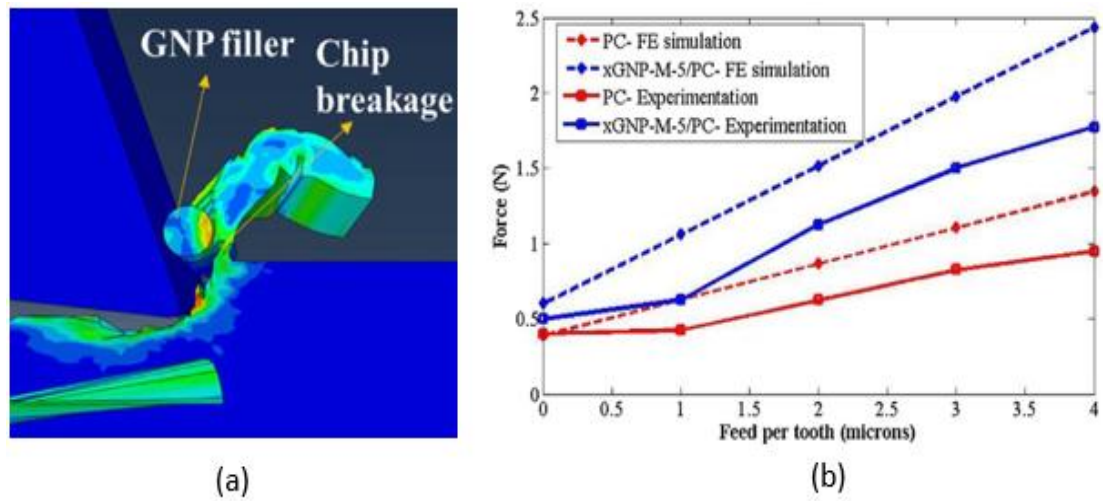


Figure 29: Finite element analysis of micro-milling PC and PC reinforced GNP nanocomposite: (a) Chip formation of PC/GNP, (b) Cutting forces in simulation and experiment (Reprinted from [46] Copyright 2017, with permission from Elsevier)

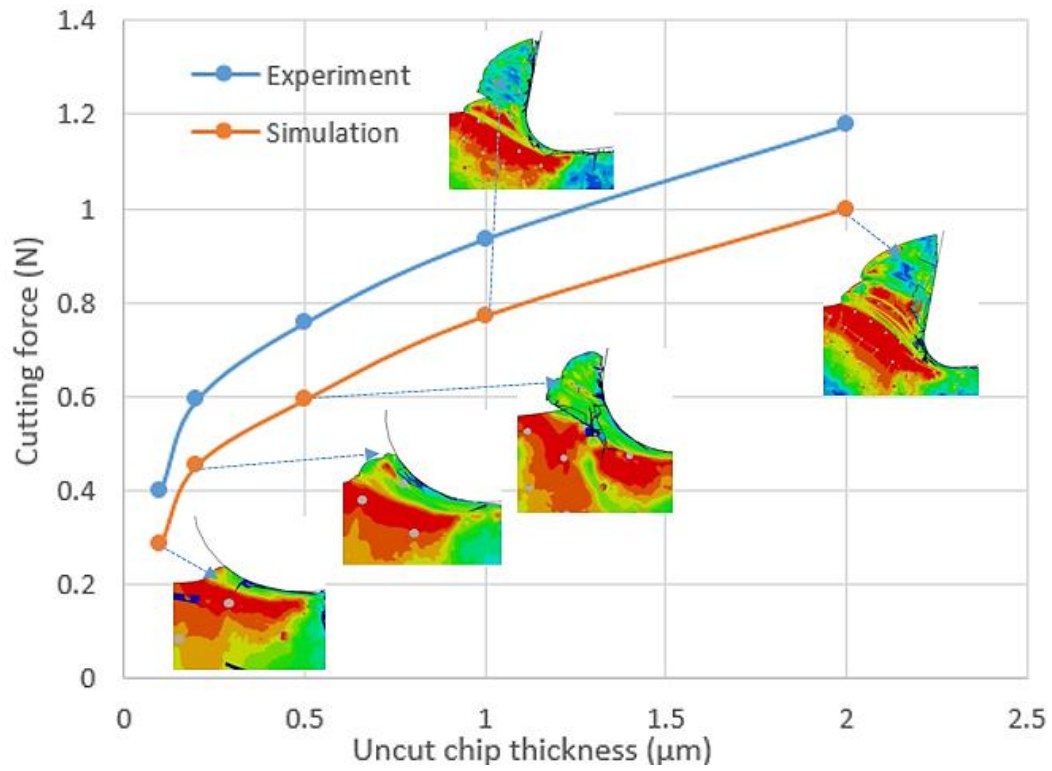


Figure 30: Finite element analysis of micro-milling Mg reinforced by 1.5 vol.% SiC nanocomposite (Reprinted from [71] Copyright 2018, with permission from The Society of Manufacturing Engineers)

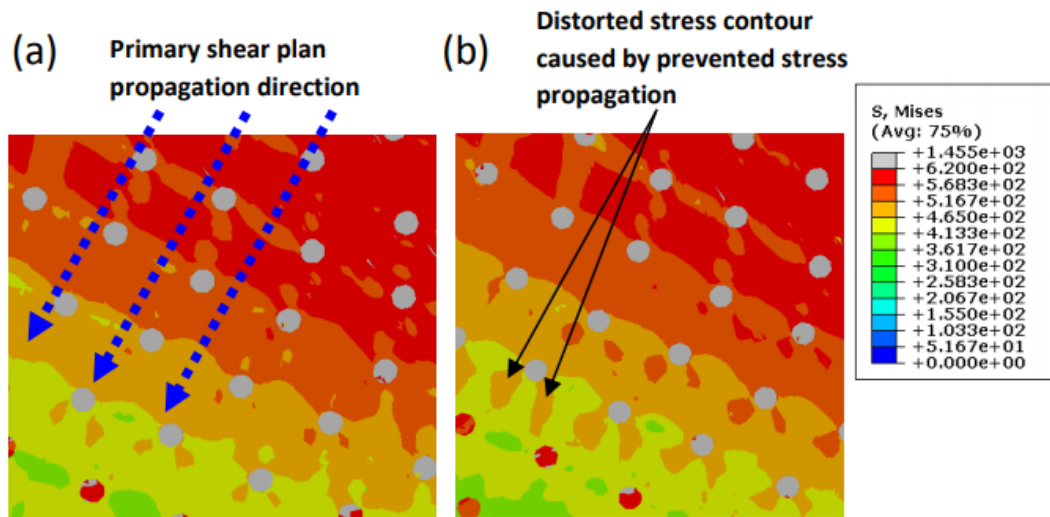


Figure 31: Effect of nano-particles on shear zone propagation: (a) direction of shear zone propagation, (b) distorted stress contour caused by particle restricting behavior (Reprinted from [96] Copyright 2018, with permission from Elsevier)

Table 1: The MUCT effects in micromachining – Relevant researches

Approach	Remarks	Ref.
Micro-milling lead, aluminum, and mild steel.	The critical depth of cut ranging from 0.1 to 0.23 mm along with different edge radius (from 0.025 into 0.06 in), and a neutral point angle 37.6° at cutting speed of 240 mm/min.	[101]
Ultra-precision turning aluminum alloys	The MUCT is 0.05-0.2 μm while the cutting edge radius is 0.2-0.6 μm	[102]
MD simulation turning aluminum, cooper	MD simulation of chip formation in copper/ aluminum cutting at 200m/s with cutting edge of 5nm exhibited the MUCT of 0.2 nm	[103]
FE simulation micro-milling ductile iron	The estimated MUCT/edge radius ratios of pearlite and ferrite are 0.2 and 0.35 respectively at the cutting speed of 110,000 rpm.	[20]
Micro-milling pure copper 101	Various cutting speed (40, 80, and 120m/min), feed-rate (0.75, 1.5,3, and 6 $\mu\text{m}/\text{flute}$), and DoC of 30 μm . Highest burr formation, largest tool wear and cutting forces were shown at the lowest ratio of feed rate/edge radius (approximately 0.4).	[104]

Table 2: Summary of micromachining CNT reinforced polymer matrix nanocomposites

Inputs						Outputs						Ref.
CNTs			Cutting condition		Tool	Chip	Cutting force	Surface roughness	Dimension accuracy	Tool wear	Burr	
Type	Loading	Direction	Feed	Speed								
--	--	--	X	--	--	X	X	X	X	--	--	[46]
Conclusions						Reasons						
High cutting force, dimensional accuracy and surface roughness when micro-milling PC/CNT with discontinuous chip forms, especially at high feed rates.						The improvement of thermo-mechanical properties due to the presence of CNT leading to strengthening-dominated and thermal-softening-neglected regimes when micro-milling PC/CNT nanocomposite.						
--	--	--	X	--	--	X	X	X	--	--	--	[45]
Conclusions						Reasons						
Continuous, curly and smooth chip forms when micro-milling PC/CNT nanocomposites as compared to broken forms with adiabatic shear bands in case of plain PC chips						Adding CNT reduce friction coefficient along the rake face and the effect of thermal softening in contrast with BUE formations due to poor thermal conduction of plain PC						
High surface quality when micro-milling PC/CNT nanocomposite						Improvement of thermo-mechanical properties due to the addition of CNT into the PC matrix. CNT infestation and polymer smearing on machined surfaces						
Low cutting force when micro-milling PC/CNT nanocomposite, especially at high feed rates						Low-quality bonding of PC-CNT leading to the reduction of failure shear strength along with the interface areas						
--	--	X	X	--	--	--	X	--	--	--	--	[51]
Conclusions						Reasons						
Higher cutting forces when micro-milling PC/MWCNT nanocomposite than that of plain PC only at low feed rate (2 μm)						Strengthening-dominated and microstructure effects associated with ploughing cutting mechanism when micro-milling PC/CNT below MUCT.						
Significant increase of cutting force when micro-milling in inflow direction in comparison with that of cross-flow direction						Stress concentration and crack formation ahead of the tooltip due to CNT agglomeration						
--	--	--	X	X	--	--	--	X	--	--	--	[52]
Conclusions						Reasons						
Surface roughness decreased as cutting speed decreased and feed rate decreased with the more dominant effect of feed rate when micro-milling HDPE/MWCNT						Visco-elasticity nature of HDPE matrix and feed marks						
--	X	--	X	X	--	X	X	X	--	--	X	[44]
Conclusions						Reasons						
The feasible chip formation when micro-milling PC/CNT nanocomposites at low feed rate (below tool edge radius).						Reinforcing CNT changed the stress-strain behavior of PC based materials, exhibiting by the reduction in strain-to-failure that indicated a ductile-to-brittle transition						
High surface quality and low burr width when micro-milling PC/CNT nanocomposite.						Addition of CNTs that leads to thermal conductivity improvement of nanocomposite						
Cutting force exhibited significant reduction when increasing cutting speed regardless of the filler content						The thermal softening-dominated regime of micromachining PC, low-loading CNT nanocomposites and crack propagation from low interfacial bonding of CNT-PC when adding higher loading of CNT.						

Table 3: Summary of micromachining graphene reinforced polymer matrix nanocomposites

Inputs					Outputs						Ref.
Graphene		Cutting condition		Tool	Chip	Cutting force	Surface roughness	Dimension accuracy	Tool wear	Burr	
Type	Loading	Feed	Speed								
--	X	X	X	--	X	X	X	--	X	--	[54]
Conclusions					Reasons						
Reduction of MCT with GPL addition					Ductile-to-brittle transition when adding GPL into epoxy						
Highest cutting forces at 0.2 wt.% GPL					Most effective reinforcement of GPL in terms of mechanical properties						
Cracks and debris on the machined surface at high content of GPL					Agglomeration of GPL, low interfacial interaction of GPL-epoxy leading to a strength-to-failure reduction						
Optimum tool wear at 0.2 wt.% GPL					Lubricant effect of GPL at the tool-chip interface and its role in minimizing sliding of polymer chains, subsequently reducing rubbing on the tool clearance face.						
--	--	X	X	--	X	X	X	--	X	--	[49]
Conclusions					Reasons						
Low cutting force, surface roughness and tool wear when adding GPL into Epoxy/GF system					Improvement of thermal conductivity and lubrication at the tool-chip interface lead to BUE reduction and tool wear Shearing-dominated regime due to superior interface strength of GPL-epoxy, leading to low glass fiber extrusion on the machined surface.						
The sensitive influence of cutting speed on surface quality improvement regardless of the material types					The dominance of strain hardening effect at high cutting speeds						
X	--	X	--	--	X	X	X	X	--	--	[46]
Conclusions					Reasons						
Discontinuous chip formation, high surface quality and cutting forces when micro-milling PC/GPL					Reduction of BUE due to the improvement thermo-mechanical properties when adding GPL filler into PC matrix						
--	X	X	X	--	--	X	X	--	X	--	[56]
Conclusions					Reasons						
Highest cutting forces at 0.5wt.% GPL with the dominance of feed rate instead of cutting speed.					Most effective reinforcement of GPL in terms of mechanical properties of epoxy/GPL leads to mechanical strengthening dominance when micro-milling epoxy/GPL						

Table 4: Summary of micromachining nano-ceramic-particles reinforced metal matrix nanocomposites

Inputs						Outputs						Ref
Material	Filler loading	Cutting condition			Tool	Chip	Cutting force	Surface roughness	Dimension accuracy	Tool wear	Burr	
		Feed	Speed	DoC								
Mg/SiC	X	X	X	--	--	--	X	--	--	--	--	[58]
Conclusions						Reasons						
Non-linear increase of specific cutting energy when reducing feed rate below MUCT.						Size effect in micromachining						
Wider ploughing zone when micro-milling Mg/SiC indicates higher MUCT with more SiC content						The predominance of thermal softening due to the reduction of thermal conductivity when micro-milling Mg/SiC at low feed rates						
Higher specific cutting forces when micro-milling Mg/SiC in ploughing zone						Strengthening effect and microstructure effect of inhomogeneous nanocomposite						
Highest cutting forces when micro-milling Mg/SiC (10 vol %).						Improvement of yield strength and fracture strength due to SiC addition						
Complex force profiles of micro-milling Mg/SiC						Microstructure effect						
Mg/SiC	X	X	X	--	--	--	X	X	--	--	--	[59]
Conclusions						Reasons						
The predominance of filler contents on cutting forces, especially at 5-10 vol% of SiC						Improvement of mechanical properties when adding more SiC in Mg matrix						
Unremarkable effect of feed rate on surface roughness while unobvious correlations between filler content-cutting speed and surface roughness were seen.						Complex micro-cutting mechanism while tool deflection and microstructure are also dominant						
Mg/TiB ₂ Mg/Ti	--	X	X	X	--	--	X	X	--	X	--	[60]
Conclusions						Reasons						
High tool wear rate when micro-milling Mg/TiB ₂ with tool coating peeling						High mechanical properties and thermal load of Mg/TiB ₂						
Higher cutting force when micro-milling Mg/Ti than Mg/TiB ₂						Chip adherence effect in case of micro-milling Mg/Ti						
Higher surface quality when micro-milling Mg/TiB ₂ than Mg/Ti						Lower cutting forces when micro-milling Mg/TiB ₂						
In the shearing region, cutting forces increased with DoC and feed rate						More resistance on tool-chip interface due to higher contacting surface						
Cutting speed and DoC have more dominant effects on surface roughness than the feed rate						The thermal softening effect when changing cutting speed and DoC						
Al/TiB ₂	--	X	X	X	--	--	X	--	--	--	--	[61]
Conclusions						Reasons						
Feed rate has the most dominant effects on cutting force when micro-milling Al/TiB ₂						Shear angle increase and friction angle decrease when increasing feed rate						
Al/SiC	--	X	X	--	--	X	X	X	--	--	--	[62]
Conclusions						Reasons						
Unobvious effect of nano-filler addition on machined surface quality						The absence of particle pull-out or failure when micro-milling Al/SiC						
The low predominance of feed rate effect on the surface finish at high cutting speed						Thermal softening effect						
No obvious trend of cutting speed-cutting force was seen						The dominated-regime alternation between thermal softening and strain hardening when changing cutting speed						

Table 5: Summary of micromachining of nanocomposites employing other micro-fabrication techniques

Micromachining techniques	Nanocomposites	Remarks	Ref.
Micro-drilling	Epoxy/CF/MWCNT	<ul style="list-style-type: none"> - The drilling-induced delamination was significantly reduced due to the addition of MWCNT. MWCNT provided better inter-laminar fracture toughness (>66%) and lowered delamination fracture (16%) compared to Epoxy/CF. - Thermal damage when micro-drilling was also reduced due to the high thermal conductivity improvement of nanocomposites due to the presence of MWCNT. 	[64]
Micro-drilling	Epoxy/CF/CNF	<ul style="list-style-type: none"> - Reduction of thrust force when using high contents of CNF reinforcement. - Increasing CNF content also led to a reduction of delamination factor since it provided better inter-laminar bond strength with the matrix. - Thrust force and delamination increased when increasing the feed and reducing the speed. Therefore, a combination of high cutting speed and low feed was recommended to minimize delamination. 	[65]
Laser micromachining	HDPE/CNF	<ul style="list-style-type: none"> - The additional of CNFs significantly enhanced the polymer decomposition, hence improving the ablation process. 	[67]
Laser micromachining	Epoxy/BaTiO ₃	<ul style="list-style-type: none"> - Suitable surfaces of thin-film based Epoxy/BaTiO₃ nanocomposites could be manufactured using laser micromachining at a wavelength of 355 nm. 	
Laser micromachining	Fe/Al ₂ O ₃ /CNT	<ul style="list-style-type: none"> - High thermal conductivity, small grain size and low light transmittance of high-CNT-content nanocomposites provided good machinability in terms of machined surface, microstructural integrity. 	[105]
Micro-EDM	PMMA/MWCNT	<ul style="list-style-type: none"> - Micro-EDM using PMMA/MWCNT nanocomposite at 10-35 wt.% nano-filler was feasible with proper machining conditions. - Low MWCNT loadings and high input voltage were recommended to achieve high dimensional accuracy as well as surface roughness. 	[106]